



**HAL**  
open science

## High human influence on beach response to tropical cyclones in small islands: Saint-Martin Island, Lesser Antilles

Virginie Duvat, Valentin Pillet, Natacha Volto, Yann Krien, Raphaël Cécé,  
Didier Bernard

### ► To cite this version:

Virginie Duvat, Valentin Pillet, Natacha Volto, Yann Krien, Raphaël Cécé, et al.. High human influence on beach response to tropical cyclones in small islands: Saint-Martin Island, Lesser Antilles. *Geomorphology*, 2019, 325, pp.70-91. 10.1016/j.geomorph.2018.09.029 . hal-01924514

**HAL Id: hal-01924514**

**<https://univ-rochelle.hal.science/hal-01924514v1>**

Submitted on 11 Jan 2019

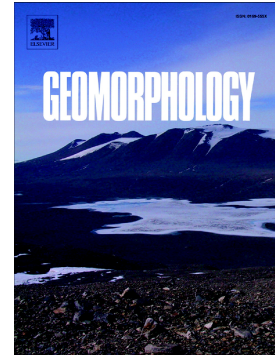
**HAL** is a multi-disciplinary open access archive for the deposit and dissemination of scientific research documents, whether they are published or not. The documents may come from teaching and research institutions in France or abroad, or from public or private research centers.

L'archive ouverte pluridisciplinaire **HAL**, est destinée au dépôt et à la diffusion de documents scientifiques de niveau recherche, publiés ou non, émanant des établissements d'enseignement et de recherche français ou étrangers, des laboratoires publics ou privés.

## Accepted Manuscript

High human influence on beach response to tropical cyclones in small islands: Saint-Martin Island, Lesser Antilles

Virginie Duvat, Valentin Pillet, Natacha Volto, Yann Krien, Raphaël Cécé, Didier Bernard



PII: S0169-555X(18)30399-4  
DOI: doi:[10.1016/j.geomorph.2018.09.029](https://doi.org/10.1016/j.geomorph.2018.09.029)  
Reference: GEOMOR 6538  
To appear in: *Geomorphology*  
Received date: 2 March 2018  
Revised date: 28 September 2018  
Accepted date: 30 September 2018

Please cite this article as: Virginie Duvat, Valentin Pillet, Natacha Volto, Yann Krien, Raphaël Cécé, Didier Bernard , High human influence on beach response to tropical cyclones in small islands: Saint-Martin Island, Lesser Antilles. *Geomor* (2018), doi:[10.1016/j.geomorph.2018.09.029](https://doi.org/10.1016/j.geomorph.2018.09.029)

This is a PDF file of an unedited manuscript that has been accepted for publication. As a service to our customers we are providing this early version of the manuscript. The manuscript will undergo copyediting, typesetting, and review of the resulting proof before it is published in its final form. Please note that during the production process errors may be discovered which could affect the content, and all legal disclaimers that apply to the journal pertain.

**High human influence on beach response to tropical cyclones in small  
islands: Saint-Martin Island, Lesser Antilles**

**Virginie DUVAT<sup>1</sup>, Valentin PILLET<sup>1</sup>, Natacha VOLTO<sup>1</sup>, Yann KRIEN<sup>2</sup>,  
Raphaël CÉCÉ<sup>2</sup>, Didier BERNARD<sup>2</sup>**

<sup>1</sup>UMR LIENSs 7266, University of la Rochelle-CNRS, 2 rue Olympe de Gouges, 17000 La Rochelle, France

<sup>2</sup>EA 4539 LARGE, University of the French West Indies, Fouillole Campus, Guadeloupe, France

**Abstract**

Using multi-date satellite imagery and field observations, this paper assesses the inferred impacts of September 2017 cyclones on the beaches of Saint-Martin Island. Twenty-two beaches out of 30 predominantly exhibited shoreline retreat, with the highest retreat value (–166.45 m) recorded on the north-eastern coast. While erosion predominated on beaches and at the sand dune front, inner areas generally exhibited accretion, with sand sheets (up to 135 m from the pre-cyclone vegetation line) indicating landward sediment transfer. Natural back-reef beaches exhibited the formation of new beach ridges, marked (up to 2 m) upward growth and alongshore beach extension. The high spatial variability of inferred impacts is attributed to the cyclone's track, coast exposure, beach configuration and, importantly, human-driven environmental change. Whereas vegetation removal exacerbated marine inundation and inhibited the vertical accretion of beaches, shoreline hardening aggravated wave-induced sediment loss while also inhibiting sediment deposition. Four beach response modes are distinguished. Based on findings, we identified three major areas of action for risk reduction and adaptation to climate change. Depending on beach response and site specificities, relocation and the determination of set-back lines, coastal buffer restoration, or engineered structures' upgrading should be prioritized.

# **High human influence on beach response to tropical cyclones in small islands:**

## **Saint-Martin Island, Lesser Antilles**

### **1. Introduction**

Tropical cyclones (TCs) have four categories of impacts on small islands (Nurse et al., 2014; Duvat et al., 2016). The first category involves morphological impacts, including coastal erosion and accretion, with erosional effects predominating along some shorelines, while others are mainly subject to sediment deposition (Hubbard et al., 1991; Scoffin, 1993; Scheffers and Scheffers, 2006; Caron, 2011; Etienne, 2012; Duvat et al., 2016; Mahabot et al., 2017); flooding and marine inundation (De Scally, 2008, 2014; Etienne, 2012; Duvat et al., 2016; Rey et al., 2017); and significant changes in island morphology, especially as a result of river action and landslides (Terry et al., 2002; Etienne, 2012). The second category comprises impacts on ecosystems and natural resources, including coral reef mortality, due to mechanical destruction, river runoff, and a decrease in coral recruitment (Bythell et al., 1993; Crabbe et al., 2008; Fletcher et al., 2008; Scopéltis et al., 2009; Mallela and Crabbe, 2009), damage to mangroves, wetlands and terrestrial forests (Cahoon et al., 2003; Park et al., 2009; Imbert and Portecop, 2008), and soil and freshwater lens salinization (Terry and Falkland, 2010; Strobl, 2012). The third category involves impacts on island livelihoods, i.e. damage to subsistence crops and fish production (Richmond and Sovacool, 2012), and losses in commercial activities, i.e. agriculture, tourism and aquaculture (OECS, 2004; Angelucci and Conforti, 2010). Lastly, the fourth category covers impacts on settlements and infrastructure, including damage to buildings (Etienne, 2012; Ferdinand et al., 2012; Duvat et al., 2016; Rey et al., 2017), public and transport facilities, and health infrastructure (Dorville and Zahibo, 2010; Richmond and Sovacool, 2012).

With the exception of geomorphic studies that explored the relationship between morphological impacts and impacts on ecosystems, e.g. provision of sediments by the reef to the coast (e.g. Etienne, 2012; Etienne and Terry, 2012; Perry et al., 2014; Duvat et al., 2017a), few studies have investigated the linkages between these four categories of impacts, i.e. the “cascades of impacts” that explain the high vulnerability of small islands to TCs. In particular, studies on morphological impacts mainly focused on the physical determinants of the latter, and especially highlighted (i) the major control exerted by coast exposure to wave action vs. proximity to the landfall path (Perry et al., 2014; Duvat et al., 2016; Mahabot et al., 2017); (ii) the high spatial variability of accretional and erosional impacts on island and sediment cell scales (Caron, 2011; Etienne, 2012; Etienne and Terry, 2012; Perry et al., 2014; Duvat et al., 2016); (iii) the major role of local topography and bathymetry in driving the nature and intensity of impacts (McIntyre and Walker, 1964; Mahabot et al., 2017); (iv) the control exerted by reef width on beach response (e.g. Mahabot et al., 2017); (v) greater destruction of introduced compared to indigenous vegetation, accounting for contrasting (i.e. higher in the former case vs. lower in the latter) erosion rates (Stoddart, 1971; Duvat et al., 2017a). Likewise, the studies conducted on Caribbean islands especially highlighted the high spatial variability of impacts and the major contribution of intense TCs, i.e. Hugo (1989), Luis (1995), Lenny (1999), Dean (2007) and Omar (2008), to marked (from  $-3$  to  $-18$  m) and permanent shoreline retreat (Cambers, 1997, 2009; Martin and Mompellat, 2000; Chauvet et al., 2007; Chauvet and Joseph, 2008). Curiously, previous studies paid little attention to the control exerted by human-driven environmental change (especially building and infrastructure construction) on coastal systems’ response to cyclonic events. Yet, because TCs impacts are highly influenced by anthropogenic controls on developed coasts, assessing the implications of the latter on coastal systems’ response is urgently required, first for improving knowledge on the vulnerability of small islands’ coastal areas to TCs, and second for designing

appropriate (i.e. site-specific) risk reduction and adaptation to climate change policies (Burningham and French, 2017; Mycoo, 2017).

Based on the assessment of the morphological impacts of September 2017 category 4 and 5 TCs Irma, José and Maria, on the sedimentary coasts (i.e. beaches and barrier beaches) of the developed island of Saint-Martin, Lesser Antilles, this paper addresses this major research gap. Based on multi-date satellite image analysis and on post-cyclone fieldwork, it builds on the opportunity provided especially by TC Irma (916 hPa) to characterize the impacts of such an intense TC on beach sites exhibiting highly contrasting (i.e. from natural to highly modified) human-driven environmental change. It more specifically addresses two key questions: (1) to what extent did human-driven environmental change influence beach response to September 2017 TCs, and (2) what lessons can be learnt from the impacts of these cyclones for risk reduction and adaptation to climate change policies?

## **2. Context of the study**

### **2.1. Study area**

#### **2.1.1. Main physical features**

The island of Saint-Martin is situated at the northern end of the Lesser Antilles Arc, which constitutes the emerged part of a vast tectonic structure located at the eastern end of the Caribbean plate (Westercamp and Tazieff, 1980). This structure includes twenty main islands stretching 900 km from north to south, and extending from 11°58'N to 18°15'N (Fig. 1). Saint-Martin is a medium-size (93 km<sup>2</sup>) island, which is roughly triangular in shape and has maximal dimensions of 13 km and 15 km from north to south and from west to east, respectively (Fig. 2). The island has a highly contrasting topography with steep slopes, and consists of four geological formations (Ramalho, 1971; Solomiac, 1974; Andreieff et al., 1988): (1) the Pointe Blanche sedimentary formation, of Eocene age and made of limestone rocks, which peaks with Pic du Paradis at 424m above sea level and forms rocky cliffs on the northern, eastern and

southern coasts; (2) the Oligocene (30 to 36 My) intrusive formation mainly made of diorite, andesites and basalts, forming cliffs along the eastern, southern and south-western coasts; (3) the Oligo-Miocene Terres Basses sedimentary formation, made of limestone and marl, which forms most of the western peninsula; and (4) a Quaternary sediment formation from alluvial and marine origin, which has filled the inner areas separating rocky headlands. At the coast, the latter forms two types of very low-lying areas, namely beaches backing onto coastal plains or mountainous slopes, and barrier beaches associated with muddy lagoons, some of which are bordered by mangrove forests (Table 1). Elevations are <5 m on 25% of the island's land area (DDE Guadeloupe, 2008), with beaches and barrier beaches being very low-lying and rarely bordered by sand dunes. The beach material is mainly composed of sediments derived from *Halimeda* and other calcareous algae provided by algal reefs, coral fragments representing less than 10% of beach sediments (Battistini and Hirschberger, 1994). Fringing reefs are restricted to the north-eastern coast, making most beaches highly exposed to cyclonic waves (Fig. 2). The climate of the northern Lesser Antilles is tropical. The trade winds are the prevailing surface wind pattern all year long, and generate dominant winds and waves from the east-northeast to southeast. Wave heights in the area generally do not exceed 3 m, except during the cyclonic season or the winter, when atmospheric depressions in higher latitudes generate long and powerful northern swells (Cooper et al., 2013). The mean tidal range is small, averaging 0.20 m. Of note, the rainfall in Saint-Martin Island is relatively sparse between January and July. It is more significant the rest of the year, leading to an average annual rainfall reaching 1,216 mm over the 1986-2000 period at Marigot (Météo-France, 2005). During the Boreal summer, the Lesser Antilles are exposed to tropical depressions, most of which form in the Cape Verde area and track to the west-north-west to reach the Caribbean islands. On average, twelve tropical depressions reach the Caribbean region per year, six of which reaching the cyclone stage (Météo-France, 2005). The northern Lesser Antilles, including Saint-Martin



Island, were devastated by category 5 tropical cyclone Donna on 15 September 1960 and by category 4 cyclone Luis on 15 September 1995. Since then, they have been affected by two tropical cyclones, Lenny and Omar in 1999 and 2008, respectively, which were less intense than Donna and Luis. Tropical cyclone Luis in 1995 was the first TC to cause very extensive damage to human assets in coastal areas (Duvat and Magnan, 2014).

### **2.1.2. Human context: rapid population growth and coastal urbanisation**

The island has a total population of around 75,000 inhabitants, 47% of whom (36,500 inhabitants in 2013) live on its French side, while 53% (around 39,700 people) live on its Dutch side. Additionally, it hosts more than 2,400,000 tourists yearly (INSEE, 2013). The population of the island has multiplied by five since the late 1970s, as a result of rapid tourism development boosting mass immigration, including illegal immigration. Saint-Martin's reputation as a tax haven played a major role in tourism development and associated mass immigration, especially on the French side of the island where the population multiplied by 3.5 in 8 years (from 8,000 inhabitants in 1982 to 28,500 inhabitants in 1990), following the adoption of the Pons Law in 1986 (Duvat and Magnan, 2014). This brutal change in population numbers and economic activities led to the rapid and uncontrolled urbanization of low-lying coastal areas, including barrier beaches, and to the reclamation of inner lagoons for infrastructure development (Dutch international and French domestic airports), tourist development and housing purposes (Table 1 and Fig. 2). This led to the clearing or removal of the coastal indigenous vegetation mostly made of *Coccoloba uvifera*, which has generally been replaced by introduced species, mainly coconut trees (Monnier, 1987). This has exacerbated human vulnerability to cyclone-generated waves, all the more that housing is still partly made of slums built by illegal immigrants in flood-prone areas (e.g. Sandy Ground, Quartier d'Orléans). The Natural Disaster Prevention Plan of Saint-Martin (DDE Guadeloupe, 2008) classifies most of the northern and eastern urbanized barrier beaches (i.e. Nettle, Marigot, La

Potence, Grand Case, and Orient Bay, see Fig. 2) as highly exposed to cyclone-induced marine inundation, due to their very low elevation. In general, buildings have been established on upper beaches, i.e. at a very short distance from the sea, which has encouraged the construction of protection structures, which have then contributed to the modification of physical processes (Duvat, 2008). Three beach types can be distinguished depending on the level of disruption of physical processes by coastal development, namely natural (limited if no disturbance), partially disturbed and highly disturbed (Table 1). Additionally, the alteration of the lagoon environment (e.g. reclamation, obstruction of outlets, destruction of *Rhizophora* and *Avicennia* mangrove forests) has aggravated the flood risk, making low-lying barrier beaches increasingly exposed not only to marine inundation, but also to lagoon overflowing.

## **2.2. Tropical Cyclones Irma, José and Maria (September 2017)**

During the 2017 North-Atlantic cyclonic season, 17 storms, 10 hurricanes and 6 major hurricanes were observed. This season was characterized for the Lesser Antilles by three extreme hurricanes, Irma, José and Maria, associated with extreme sustainable wind speed values reaching or exceeding 250 km/h (Figs. 3a-c). The main features of these hurricanes are summarized in Table 2.

Category 5 TC Irma was born west of the Cape Verde islands (Degrace, 2017). Upon its arrival on the Lesser Antilles Arc on 6 September 2017, sustainable wind speed values were close to 296 km/h and wind gusts were estimated at 361 km/h. These extreme eyewall winds devastated the island of Barbuda before hitting Saint-Bartholomew, Saint-Martin and Anguilla on the early morning of 6 September. Irma was the first recorded TC crossing the Lesser Antilles islands with such powerful winds. Due to the heavy induced damages, very limited meteorological observational data could be collected in Saint-Martin and Saint-Bartholomew during this event. To compensate for the lack of in-situ data, and to have spatial-temporal meteorological fields to understand the impacts, an atmospheric simulation was effected with the WRF ARW model

(Skamarock et al., 2008) and a 0.4 km-resolution domain to take into account the complex shorelines of a 15 km-wide island like Saint-Martin (Cécé et al., 2014). The 6-hourly ECMWF operational analyses with  $0.1^\circ$  scale were used as initial and boundary conditions. The results (Fig. 3c) show maximum surface winds on the Atlantic side of Saint-Martin with huge gusts of 341 km/h. The maximum simulated wind speed on the coast of Saint-Martin reached 305 km/h. Based on the simulation results, the coastal areas affected by the strongest winds (above 280 km/h) were Nettle Bay, Grandes Cayes, Oyster Pond and the Terres Basses coasts from Baie Aux Cayes to Baie aux Prunes.

As there are no meteorological buoys in the area of Saint-Martin, no direct wave observation is available. Using bathymetric data from navigational charts provided by the SHOM (French Navy Hydrographic and Oceanographic Service), as well as wind fields obtained by blending CFSR data with empirical laws, we estimated that the significant wave heights ( $H_s$ ) exceeded 5 m off the coasts of Saint-Martin (Fig. 3d). The eastern coast was the most exposed, with  $H_s$  reaching 9 m. Our results suggest that the northern and southern coasts were also impacted, but with significant differences depending on the location. West-facing coasts were presumably much less exposed, since the winds were offshore during the peak of the storm. A description of SCHISM-WWM, the wave-current coupled numerical model used here, can be found in Krien et al. (2017). The tide gauge of Marigot city on the northern coast recorded a surge of 2 m. This value is consistent with the results of our storm surge numerical model, which also indicates that the water level might have reached 5 m above mean sea level locally on the eastern coast, for example in Embouchure Bay.

Three days after Irma, category 4 tropical cyclone José passed to the north at some 130 km from Saint-Bartholomew and Saint-Martin (Fig. 3a), without causing significant damage. The maximum significant wave heights still reached about 5 m off the eastern coast of Saint-Martin, according to the numerical results obtained with SCHISM-WWM (Fig. 3d-right), but the

southern and northern coasts were relatively spared. The last of these three cyclones, Maria, was considered at first as an event with a relatively low level of threat. Yet it rapidly intensified into a major hurricane off the coasts of Martinique, and reached the category 5 just before landing on Dominica, where it caused catastrophic damage. In the morning of 19 September, Maria headed towards Porto Rico, keeping a distance greater than 150 km from Saint-Martin Island, where the impacts were hence moderate.

### **3. Materials and methods**

#### **3.1. Shoreline change assessment**

##### **3.1.1. Image acquisition and preparation**

High-resolution (0.5 m) Pléiades satellite images were used in this study, which were obtained from Airbus Defence and Space (Table 3). These images were taken on 12 February 2017 (i.e. 7 months before the TCs), and on 10 and 14 September 2017 (i.e. a few days after TCs Irma and José affected the island). Limited image availability constrained the characterization of the pre-cyclone situation. Two complementary investigations were conducted to verify if the February 2017 images could be used as a benchmark of pre-cyclone shoreline position and beach status. The extraction of time series of significant wave heights from the wave global model of Ifremer (<ftp://ftp.ifremer.fr/ifremer/ww3/HINDCAST/GLOBAL/>) at two different points, located in the vicinity of Saint-Martin (see SM1), shows that only moderate northern swells with significant wave heights lower than 4 m may have had an impact on shoreline change between February and September. Since Saint-Martin is well protected from these swells by Anguilla, it is very unlikely that the changes observed between the “pre” and “post”-storm images are not due to September 2017 TCs. Therefore, we considered that the February 2017 image could be used as a benchmark to characterize the “pre-cyclone” situation. Due to important post-cyclone cloud cover constraining image analysis, two different images (10 and 14 September 2017) were used to assess the post-cyclone situation. The comparative analysis

of the February 2017 and post-cyclone images thus allowed assessment of the inferred impacts of TCs Irma and José on Saint-Martin Island. Although they were provided orthorectified by Airbus Defence and Space, these images had offsets up to 5.5 m in longitude and latitude in relation to the IGN (National Geographical Institute) orthophotography of 2013, which was therefore used to georeference them. Georeferencing was operated in ArcGIS 10.5, using a spline transformation and permanent geomorphic (headlands and beach rock slabs) and human features (major infrastructures, e.g. harbours) as ground control points.

### **3.1.2. Shoreline interpretation, digitization and analysis**

In line with recent studies assessing tropical cyclone impacts on shoreline position and coastal morphology in small islands (Duvat and Pillet, 2017; Duvat et al., 2017a, 2017b), we used the stability line as a shoreline proxy for the seaward boundary of stabilized coastal areas. This line corresponds to the edge of the vegetation in unbuilt areas and to the outer limit of coastal constructions (i.e. property walls, engineered structures...) in settled areas (Figs. 4a, 4b). While this indicator was easily detectable on the February 2017 image, it was more difficult to digitize on the post-cyclone images, due to extensive vegetation destruction. In many cases, the first vegetation line was wiped out by the cyclonic waves, which only left scattered and highly deformed trees and bushes in place. Of note, the latter were excluded from the vegetation line (Fig. 4d). Additionally, in line with previous studies (Biribo and Woodroffe, 2013; Mann and Westphal, 2014; Duvat and Pillet, 2017; Duvat et al., 2017a), we digitized the base of the beach (Figs. 4c, 4e) where it was detectable on the 12 February 2017 and 14 September 2017 images. This indicator provides valuable information on beach response to cyclonic waves, which may be either accretional or erosional (Scoffin, 1993; Duvat et al., 2016). Despite the major interest in using this shoreline indicator in complement to the stability line, its detection was made difficult at most beach sites, either by cloud cover or by wave breaking. As a result, this indicator was only digitized for four north-eastern (Petites Cayes Bay, Petites Cayes Beach,

Grandes Cayes Beach) and eastern beaches (Embouchure Bay) (Fig. 5). Shoreline change was calculated using the Digital Shoreline Analysis System (DSAS) (Thieler et al., 2009), based on the generation of 10 m-interval transects from the baseline. The Net Shoreline Movement (NSM), measuring the distance between the oldest and the most recent shorelines, was automatically generated, as in previous studies (Duvat et al., 2017a).

### 3.1.3. Uncertainty

As in previous studies, three sources of uncertainty were considered, which relate to image resolution, image georeferencing and shoreline digitization (Yates et al., 2013; Duvat et al., 2017b). The errors generated were estimated to be equal to 0.5 m (pixel size) for image resolution, ranging from 0.37 m (12 February 2017 image) to 0.67 m (14 September 2017 image) for georeferencing, and respectively  $<1$  m and  $<2$  m for the digitization of the stability line and of the base of the beach. The 2 m uncertainty considered for the digitization of the base of the beach includes the uncertainty introduced by differences in the tidal level (i.e. 1 m max.), which were of 0.17 m between the 12 February and 10 September 2017 images, and of 0.25 m between the 12 February 2017 (0.45 m) and 14 September 2017 images. Differences in tidal level had limited impacts on the digitization of the base of the beach because the latter (corresponding to the seaward limit of dense sand) was easily detectable on study sites. Of note, beaches exhibiting constraining hydrodynamic conditions were excluded from the analysis to avoid misinterpretation. As a result, the total shoreline position error was estimated to be  $<2$  m for the stability line and  $<3$  m for the base of the beach. This means that shoreline changes  $\leq 2$  m ( $\pm 2$  m) and  $\leq 3$  m ( $\pm 3$  m) for the stability line and base of the beach respectively are not significant, therefore corresponding to stable shorelines. In contrast, changes  $>+2$  m and  $\leq -2$  m, respectively, indicate an advance and a retreat of the stability line, while changes  $>+3$  m and  $\leq -3$  m, respectively, indicate an advance and a retreat of the base of the beach. These error ranges are in accordance with results obtained in similar studies.

### **3.2. Post-cyclone field survey**

A five-day field trip was conducted on the island from 28 October to 3 November 2017, i.e. approximately seven weeks after the three cyclones hit the island. At that time, international flights just started operating again and most of the wreckage had been cleaned from roads and tracks, allowing the conduction of field investigations at all beach sites. Fieldwork was dedicated to the collection of three types of data. First, we assessed the erosional and accretional impacts of the cyclones on coastal sedimentary systems, including beaches, upper beaches, inner land areas, and sand dunes and inner lagoons where they occur. The positions of cliffs cut by cyclonic waves in the upper beach and sand dunes were geolocated and their height measured. In addition, cyclonic wreck lines and sediment deposits were mapped, and the thickness of the latter was measured. Second, we analysed the impacts of the cyclonic wind and waves on the coastal vegetation, using quantitative and qualitative parameters, including the extent of the affected area, the degree of destruction of the vegetation depending on its type (herbaceous, shrubby, woody) and origin (indigenous vs. introduced), and the main destructive agents (wind vs. waves) involved. Special attention was paid to the resistance of the vegetation, to its buffering function, and to its role in sediment trapping. Third, we assessed the impact of shoreline hardening on beach response, i.e. the influence of longitudinal engineered structures (mainly cemented seawalls and rip-raps) and vertical seaside property walls on cyclone-induced physical processes. The effects of constructions on first, sediment transfer, and second, depositional and erosional processes, were investigated in detail. At most sites, the alternation of non-built and built-up shoreline sections allowed assessment of alongshore variations in beach response, depending on the degree of disturbance of physical processes by human constructions. The spatial extent and dimensions of erosional and depositional features were systematically assessed.

### **3.3. Analysis of beach response**

Satellite image analysis and field observations were complementary to assessing the impacts of the cyclones, and to determining the main factors explaining their amplitude and spatial extent. While the former allowed measuring changes in shoreline position, field observations allowed taking stock of cyclone-generated features, measuring the amplitude of change (i.e. thickness of sediment deposits, and height of cliffs in the case of vertical ablation), and mapping the landward extent of cyclone-driven sediment deposits. The field survey allowed determining the respective importance of erosional and accretional impacts at each beach site, as most sites exhibited both erosional and accretional features, e.g. beach lowering combined with sediment deposition in inland areas. It also provided major insights on the respective roles of the coastal vegetation, depending on its type and origin, and of human-built structures, in beach response.

#### **4. Results: impacts of September 2017 tropical cyclones on beaches**

##### **4.1. Impacts on shoreline position**

###### **4.1.1. Impacts on the position of the stability line**

September 2017 TCs caused a significant retreat of the stability line at most beach sites (Table 4 and Fig. 6). Twenty-two beach sites out of thirty predominantly exhibited retreat, which was detected along 65.22% (Anse des Pères) to 100.00% (Petites Cayes Bay, Petites Cayes Beach, Orient Bay central and south, Gibb's Bay, Guana Bay, Cayes Bay, Small Bay, Bell Hill Beach) of transects. The highest retreat values (i.e. >90% of transects exhibiting retreat) were obtained on the most exposed northern and eastern coasts of the island, which also experienced the lowest average and minimum NSM values. The lowest average NSM value of -68.28 m was obtained at Orient Bay Central and South, while six additional beach sites (five of which are located on the northern and north-eastern coasts) experienced values <-30 m. The minimum NSM values were <-70 m at seven beach sites distributed between the northern (Nettlé Bay), eastern (Grandes Cayes Beach, Cul de Sac Bay and Orient Bay North and Central and South, Embouchure Bay) and southern (Simpson Bay) coasts, with Cul de Sac Bay exhibiting the



record value of  $-166.45$  m. Importantly, on the southern sites of Simpson Bay and Mullet Beach, respectively, 70.36% and 72.34% of transects exhibited retreat. In contrast, the two western and therefore more sheltered beaches (namely Longue Bay and Plum Bay) mainly showed stability, which was detected along 65.88 and 59.17% of transects, respectively. On these two sites, the minimum NSM values reached  $-12.25$  m and  $-30.18$  m, respectively, confirming the limited impacts of the cyclones. The southern bays of Great Bay and Cole Bay, which are surrounded by prominent headlands, also exhibited limited retreat, with respectively 50.00 and 55.14% of transects showing stability, against respectively 50.00 and 44.86% exhibiting retreat.

Importantly, the spatial variability of impacts was high on three different spatial scales (Figs. 6, 7 and Table 4). On the island scale, the results highlight a major contrast between the highly-exposed northern and eastern coasts, and the rest of the island. At a second level, marked differences were noted within each of these two areas. For example, on the eastern coast of the island, Dawn Beach exhibited limited retreat (average NSM value of  $-9.84$  m) compared to other sites (having average NSM values ranging from  $-22.06$  to  $-68.28$  m). In the same way, contrasting responses were observed along the northern coast, as illustrated by the limited retreat experienced by La Potence Bay and Marigot Bay (with respective average NSM values of  $-2.41$  and  $-0.95$  m, and minimum NSM values of  $-12.07$  and  $-41.60$  m) in comparison to Nettlé Bay (average and minimum NSM values of  $-21.60$  and  $-108.22$  m, respectively). While Marigot Bay and La Potence Bay predominantly showed stability (detected along 83.97 to 88.57% of transects, respectively), Nettlé Bay mainly exhibited retreat (detected along 74.80% of transects). At a third level, contrasting shoreline responses were recorded on the beach site scale, some sites showing limited variability along their shoreline (e.g. La Potence Bay, Cole Bay), while others exhibited marked variability (e.g. Nettlé Bay, Cul de Sac Bay, Orient Bay

Central and South, Simpson Bay; Fig. 7). On the latter, beach extremities generally experienced limited retreat compared to the central part of bays (e.g. Nettlé Bay, Embouchure Bay).

#### **4.1.2. Impacts on the position of the base of the beach**

As a reminder, changes in the position of the base of the beach were documented for only four highly-exposed sites situated at the north-eastern tip and along the eastern coast of the island (Fig. 5). Despite the limited number of beach sites considered, contrasting behaviours were noted (Table 5, Fig. 6). The base of the beach showed a significant advance at the north-eastern tip of the island. At Petites Cayes Beach, 72.73% of transects showed advance, while average and maximum NSM values, respectively, reached 8.26 and 21.44 m, and at Grandes Cayes Beach, 59.19% of transects accreted, while average and maximum NSM values reached 3.14 and 9.80 m, respectively. Importantly, at Petites Cayes Beach, a new beach formed, which was approximately 40 m wide and 150 m long on 14 September 2017. In contrast, at Petites Cayes Bay and at Embouchure Bay (eastern coast), the base of the beach predominantly exhibited stability (detected along 68.42 and 71.18% of transects, respectively), secondarily experiencing advance (along 21.05 and 24.12% of transects, respectively). These results are in line with previous studies highlighting cyclone-induced advance of the base of the beach (Duvat et al., 2017a). Additionally, two narrow (i.e. around 5 m-wide) beaches of the southern (i.e. Maho Bay) and western (Canonier Point) coasts disappeared as a result of sediment removal.

#### **4.1.3. Change in beach width**

As a result of the differentiated behaviours of the vegetation line (retreat) and base of the beach (stability to advance), beach width increased significantly on northern and eastern sites, from 15 m to 37 m at Petites Cayes Bay, from 8 m to 15 m at Petites Cayes Beach, from 33 m to 60 m at Grandes Cayes Beach, and from 10 to 50 m in the central part of Embouchure Bay. This means that the active, i.e. unstable, part of the beach system expanded, while its stabilized (i.e. vegetated) area contracted in turn.

## 4.2. Impacts on coastal morphology

### 4.2.1. Erosional features

Generally, erosional features predominated in the beach, upper beach and sand dune edge areas (Fig. 8 and SM2). At most sites, beach lowering was revealed by the exhumation of buildings' foundations and of previously buried beachrock slabs (Fig. 8a). The highest values of beach lowering, reaching up to 2 m locally, were observed in front of buildings and seawalls protruding onto beaches (e.g. Red Bay, Fig. 8b). Although beach recovery had started at the time of our field visit, the erosional impacts of the cyclones were still clearly shown first, by the erosion scarps cut into the upper beach (generally 0.30 to 0.80 m high) and sand dunes where the latter occur (with scarps ranging from 1.50 to 4 m in height at Longue Bay and Red Bay; Fig. 8c), and second, by the exhumation of the root system of the destroyed vegetation over a 5 to 40 m-wide coastal strip (Figs. 8d, 8e). The height of erosion scarps was proportional to land elevation, thereby varying significantly between low-lying barrier beaches, where it ranged from 0.30 to 0.60 m, and beach-dune systems, where it reached up to 4 m. In places, scour holes and soil scouring were also noted (e.g. at Petites Cayes Bay, Orient Bay, Embouchure Bay and Guana Bay; Figs. 8e, 8f), which extended from the upper beach to inner land areas over distances ranging from a few metres to around twenty metres. On the most affected eastern site, namely Orient Bay, wave attack even led to the formation of a 1.20 m-deep and 15 m-long trough, extending transversally to the shoreline from the upper beach to inner land areas (Fig. 8d).

### 4.2.2. Accretional features

While erosion predominated on beaches and upper beaches, sand accumulation prevailed in inner land areas as a result of overwash where no obstacle, neither natural (i.e. dense vegetation) nor human-built (i.e. buildings and engineered structures), obstructed sediment transport pathways. Extensive sand sheets indicating massive sediment transfer from beaches to

inner land areas were the most common feature observed (Fig. 9, SM3). In open areas, sand deposits penetrated inland over great distances, i.e. 135 m, 105 m and 75 m from the pre-cyclone vegetation line at Simpson Bay, Nettle Bay (west) and Mullet Bay, respectively (Fig. 9a). At most sites, the maximum thickness of these sand sheets ranged from 0.10 to 0.80 m (Fig. 9b). It reached the maximum value of 2 m on the highly-exposed eastern coast at Gibb's Bay (Fig. 9d). Moreover, at two sites (i.e. Red Bay and Gibb's Bay), barrier beach overwashing by the cyclonic waves caused sediment deposition in the inner lagoon, where sand lobes formed (Fig. 9c). In addition, at one site (i.e. Embouchure Bay), a new channel (maximum dimensions of 15 m x 75 m) formed across the barrier beach. Of note, on the north-eastern back-reef beaches (namely Petites Cayes Bay and Petites Cayes Beach), the substantial transfer to the coast of coral debris (primarily shingle and rubble, and secondarily blocks) led to the formation of crescent-shaped deposits at the base of the beach (Fig. 9g) and of a 0.80 m-high, 20 m-wide and 60 m-long beach ridge on the upper beach (Fig. 9e). Additionally, on highly eroded beaches bordered with beachrock slabs, the dismantling and landward transfer of fragments of the latter caused block accumulation at the beach surface and along the erosion scarps cut by cyclonic waves in upper beaches and sand dunes (Fig. 9h).

### **4.3. Influence of human-driven environmental change on beach response**

#### **4.3.1. Impact of vegetation modification**

The response of beaches varied considerably depending on the degree of vegetation modification (Table 1). Where the indigenous or mixed shrubby, i.e. dense, vegetation has been conserved, forming a continuous and relatively wide (>30-50 m) formation along the shoreline, it acted as a buffer, limiting the penetration of the cyclonic waves inland and contributing to the vertical accretion of coastal systems. Similar findings were obtained in Belize and Farquhar (Seychelles Islands) following TCs Hattie (Stoddart, 1963, 1965) and Fantala (Duvat et al., 2017a), respectively. Where the first vegetation line was either destroyed or severely damaged

by the cyclonic waves, which occurred over a distance of 10 to 30 m depending on the site, a second vegetation line resisted and buffered the cyclonic waves. It therefore prevented the propagation of marine inundation and of associated sediment deposition in inner land areas, while also causing substantial sediment trapping (Fig. 9f). This led to the formation of elevated (i.e. reaching up to 1.70 m in height) beach ridges along the shoreline. In contrast, where the native vegetation has been removed and replaced by introduced woody species (mostly coconut trees), the latter generally suffered total destruction, which, together with the absence of undergrowth, caused extensive marine inundation and sediment deposition across inland areas. In this case, no beach ridge formed, the spreading of sediment limiting vertical accretion. In addition, while the dense branch and root system of the indigenous vegetation limited soil scouring on natural coasts, modified areas having introduced and sparse vegetation suffered intense and extensive soil scouring.

#### **4.3.2. Impact of longitudinal constructions on shoreline response**

The behaviour of the stability line varied considerably, depending on the degree of shoreline modification and hardening (Table 1). In built-up areas, the degree of resistance of human constructions to cyclonic waves, which proved to be highly variable, was the major control of the stability line behaviour. In densely urbanized areas (e.g. Marigot, Grand Case and Philipsburg) and in areas equipped with major infrastructure, such as airports and critical facilities (Grand Case, Simpson Bay, La Potence Bay, Cole Bay), where the stability line corresponded to the seaward limit of human constructions or of large engineered structures, the resistance of the latter caused shoreline stability (Fig. 10a, 10b). For example, the high resistance of constructions along the entire shoreline at La Potence Bay and Cole Bay explains the low average and minimum NSM values recorded there (Table 4, Figs. 6, 7). Beach sites showing high variations in shoreline resistance, due to the alternation of built-up and non-built shoreline sections, or to variations in the resistance of seaside buildings (slums vs. resistant

buildings) and of coastal protection structures (due to variations in the materials used, size and condition of structures), exhibited not only greater average and minimum NSM values but also more contrasting values along their shoreline (e.g. Baie Nettle, Simpson Bay and Great Bay). Generally, tourist beach sites (e.g. Terres Basses, Orient Bay, Dawn Beach, Guana Bay) exhibited an intermediate situation (Figs. 10c-e), i.e. medium NSM values and limited variations of NSM values along their shoreline, due to limited variations in the resistance of buildings and coastal protection structures. There, the low-to-middle size rip-raps erected by private owners were often dismantled by cyclonic waves, accounting for the damage to houses and marked upper beach erosion (Figs. 10c-d). Where houses were wiped out by the cyclonic waves, higher retreat values were observed (e.g. Guana Bay, Fig. 10e). Collectively, these results indicate that shoreline-fixing by human constructions tends to reduce cyclone-induced shoreline movement.

#### **4.3.3. Impact of longitudinal constructions on erosional and accretional processes**

Shoreline hardening also had impacts on erosional and accretional cyclone-driven processes. Beach lowering was greater in front of seaside property walls and seawalls, where it reached up to  $-2$  m (Figs. 8b, 10c, 10d), compared to non-built shoreline sections where values  $<0.80$  m were observed. In addition, where sediment transport pathways were obstructed by human constructions, sand accumulation only occurred in devastated buildings and swimming pools (Figs. 10f-g), and in gaps between buildings (Fig. 9b). Where human constructions were continuous along the shoreline, sediment deposition on upper beaches and over inland areas was either absent or very limited (Fig. 10a). At the time of the field visit, in settled residential areas, invading sand deposits had been cleaned and raked-up into piles by residents (Fig. 10g). Longitudinal constructions therefore exacerbated the erosional impacts of the cyclonic waves on beaches, while limiting sediment deposition on upper beaches and over inland areas.

## **5. Discussion**

### 5.1. Including human-driven feedback effects in cyclone impact studies

In line with previous studies (Ford and Kench, 2014; Duvat et al., 2016; Duvat et al., 2017a, 2017b), our results highlight the high spatial variability of TCs impacts. In the present case, the latter can be attributed to four main factors. The first influential factor was the cyclone's track. Although the succession of three intense TCs within less than two weeks necessarily imposes limits in the understanding of their respective impacts, the analysis of the spatial distribution of impacts confirms that Irma was the most impacting cyclone, due both to its track (passage over the island) and to its intensity (i.e. wave height). Its track explains the greater impacts (i.e. average and minimum NSM values, extent of sand sheets) noted on the highly-exposed northern and eastern coasts of the island, compared to its more sheltered western and southern coasts. The second influential factor was shoreline exposure, which varies considerably on the island scale, depending on shoreline outline (concave vs. convex) and on the sheltering effect provided to some beaches by surrounding rocky headlands. In general, the sheltered extremities of large bays exhibited limited shoreline retreat compared to their central part and to convex shoreline sections. The third influential factor was the geomorphic configuration of beach sites. Barrier beaches bordered with inner lagoons experienced greater positional changes compared to beaches backing onto coastal plains or mountainous slopes. Additionally, while back-reef beaches showed marked accretion due to the massive transfer to the coast of coral debris and blocks provided by the reef, open beaches (i.e. having no or an embryonic and discontinuous fringing reef) exhibited limited accretion, mainly occurring in the form of sand deposition. Further, whereas beach-dune systems (reaching around 5-6 m in height) experienced marked shoreline retreat due to substantial sediment removal caused by wave breaking at the dune front, low-lying barrier beaches (<3 m) mainly exhibited widespread marine inundation associated with the formation of extensive sand sheets. These findings, i.e. the major roles of the cyclone's track, coast exposure and geomorphic configuration of beach sites in driving the

nature and intensity –and thereby the spatial variability – of TCs impacts, are in line with previous studies (McIntyre and Walker, 1964; Caron, 2011; Etienne, 2012; Etienne and Terry, 2012; Perry et al., 2014; Duvat et al., 2016; Mahabot et al., 2017).

Beyond confirming the role of these three influential factors, our study emphasizes the crucial control exerted by human-driven environmental change, especially shoreline hardening and vegetation modification, on beach response to TCs. Shoreline hardening reduced shoreline movement where human constructions resisted to the cyclonic waves. But at the same time, it exacerbated sand loss, due to increased sediment souring (due to wave reflection) and limited inland sediment deposition (due to the obstruction of sediment transport pathways), in front of human constructions. It therefore amplified the detrimental impact of the cyclones on the sediment budget of beaches. On unbuilt shorelines having introduced vegetation, marine inundation reached the inner part of coastal plains, causing sedimentation over great distances and damage to human assets. There, the removal of cyclone deposits by residents destroyed the positive impacts of the TCs. Collectively, these results show that anthropogenic interferences with physical processes, by exacerbating cyclone-induced sediment loss and reducing or destroying cyclone-induced sediment gains, increase the geomorphic vulnerability of coastal systems, which in turn exacerbates the exposure and vulnerability of coastal human assets. By altering the capacity of coastal systems to accrete as a result of cyclone-induced sediment deposition, vegetation degradation and shoreline hardening increase their vulnerability to future TCs and sea-level rise. More generally, these results highlight the feedback effects associated with “coastal squeeze”, i.e. the exacerbation of coastal risks by the compression and even suppression of buffering beach-dune and beach systems (Cooper and McKenna, 2008; Cooper and Pile, 2014). Where these human-driven feedback effects operate, impacts are not only different in nature but also more severe, compared to impacts on natural beach sites. Because human interventions influence the “cascade of impacts” of a cyclonic event, they should be



systematically considered in cyclone impact studies (Hapke et al., 2013; Duvat et al., 2016; Burningham and French, 2017; Rey et al., 2017).

## **5.2. Beach types**

In the absence of any pre-existing typology of beach response modes to TCs in tropical small island environments, the typology elaborated below builds on the above-presented results.

### **5.2.1. Responses of “natural” beach sites**

#### **Type 1: back-reef accretional beach (Fig. 11)**

In the study area, back-reef beaches backing onto coastal plains or inner reliefs underwent important sediment gains. Although they experienced both erosional (i.e. stability line retreat and localized upper beach lowering) and accretional (localized beach accretion, formation of 0.80 to 1.65 m-high beach ridges) processes, as the latter were predominant, they accreted. The indigenous vegetation played a major role in beach response: while the first line of vegetation (over a distance of 20 to 30 m) was destroyed or severely damaged, the second line of vegetation resisted, trapping coral blocks and debris, which resulted in the formation of beach ridges. One of these beaches even extended along the shoreline. To conclude, TCs have two major impacts on these beaches: they supply the beach system with sediments and considerably increase the elevation of its seaward part, thereby reducing the vulnerability of these systems to future climate-related pressures.

#### **Type 2: erosional and migrating barrier beach (Fig. 12)**

This type, here illustrated by the small (160 m x 40 m) barrier beach of Gibb's Bay, exhibited marked cyclone-induced erosion. The retreat of the stability line caused an important reduction in width (here from 40 m to 17 m) of the vegetated, i.e. stabilized, part of the barrier beach. Additionally, as a result of the cyclonic waves crossing over the barrier beach, massive ocean-to-lagoon sediment transfer occurred, leading to the advance (of 5 to 13 m here) and marked (up to 2 m) upward growth of the lagoon shoreline. As a result of ocean-facing shoreline retreat

and lagoon-facing shoreline advance, the barrier beach migrated landward. Therefore, TCs increase the vulnerability of such features to future climate-related pressures.

### **5.2.2. Responses of modified beach sites**

**Type 3: back-reef erosional beach or barrier beach affected by human disturbances (Fig. 13)**

As a result of population growth and tourist development, this beach type prevails. Barrier beaches and beaches exhibiting vegetation modification, including change from indigenous to introduced species and vegetation clearing (e.g. northern part of Embouchure Bay, Orient Bay), underwent marked shoreline retreat and sand loss (indicated by 0.30 to 1.50 m-high erosion scarps), to which vegetation modification contributed. Generally, the indigenous vegetation was either partly or entirely removed for development purposes, and replaced by an urbanized seafront providing diverse amenities (parking areas, shops, etc.). As a result, highly-exposed buildings protruding onto the beach had to be protected from wave attack by engineered structures. In such a configuration, both the amplification of cyclone-induced beach erosion and soil scouring, and of marine inundation by vegetation removal, and the suppression of cyclones' constructional impacts by the removal of sediment deposits, led to an increase in the vulnerability of the beach system and in the exposure of the human assets established in the coastal plain.

**Type 4: stable hardened beach sites (Fig. 14)**

Beach sites characterized either by a continuous line of buildings or by shoreline hardening due to the erection of large engineered structures (e.g. Marigot Bay and La Potence Bay), exhibited very limited shoreline retreat and sediment inputs, as a result of the resistance of constructions and of the obstruction of sediment transport pathways by the latter. Marine inundation was also inhibited by coastal development, only occurring in gaps between constructions. TCs therefore have limited impacts on the vulnerability of these highly-modified coastal systems.

### **5.3. Implications for risk reduction and adaptation to climate change**

#### **5.3.1. Relocating exposed human assets and determining set-back lines to reduce coastal areas' vulnerability**

Making or keeping the “cyclone wave impact zone” free from construction should be considered as a key priority in highly-damaged areas over the reconstruction phase, as this is the only option to break the undesirable human-induced feedback effects on Type 3 beach sites. This implies not only to relocating the constructions that were built in the “cyclone wave impact zone” to safer inland areas, but also to design adequate set-back lines for future constructions, including destroyed buildings and infrastructure that will be rebuilt (Burningham and French, 2017; Mycoo, 2017). Because TC Irma was the most intense TC to ever hit Saint-Martin, the spatial distribution of its impacts should be considered in urban planning. The results obtained in this study (e.g. sediment deposits reaching a maximum distance of 135 m from the vegetation line) advocate for the enforcement, on Saint-Martin Island, of the French Littoral Law imposing to keep free from construction a 100 m-wide coastal strip. The current coastal development mode proved to be unsustainable in the face of TCs.

#### **5.3.2. Preserving and restoring natural buffering areas**

Importantly, on Type 3 beach sites, making (where constructions occur) or keeping (where future constructions are envisaged) the “cyclone wave impact zone” free from construction will not be sufficient to reduce the current vulnerability of coastal areas to TCs. To secure human assets established in coastal plains and break the human-driven negative feedback effects described above imperatively requires the restoration of degraded coastal buffering areas, i.e. the morphological-ecological features that were altered by human development. This implies beach nourishment where the beach budget is in deficit, and vegetation replantation on both the upper beach and back-beach. Given its resistance to cyclonic winds and waves, and its capacity to trap sediments and contribute to coastal systems' upward growth, indigenous vegetation

should be replanted wherever it was cleared. The coastal systems that are still functional, i.e. that proved to be resilient (i.e. resistant and constructional) in the face of TC Irma, provide good examples to follow for the restoration of degraded coastal systems. In addition, where coastal buffers are still functional (on a number of “natural” beach sites), they should be strategically protected from future human degradation. Last, the valuable experience that some Caribbean countries (e.g. Cuba, Barbados) already have in the inclusion of vegetation preservation or restoration in land-use planning (Mycoo, 2017), could be shared with and potentially transferred to Saint-Martin.

### **5.3.3. Upgrading engineered structures in highly vulnerable areas**

As a reminder, the dismantling of inappropriate (i.e. either poorly designed or of inadequate type) engineered structures aggravated TCs impacts, especially in residential and tourist areas where these structures were of rustic style. Poor protection structures are common in small islands, due to limited technical and financial capacities (Nunn, 2009; Duvat, 2013), and should be replaced by proper engineered structures in areas concentrating most human assets. In such areas, the priority should be to reduce the physical exposure of anthropogenic assets to cyclonic waves. This strategy would be appropriate on developed sites where relocation cannot be envisaged or requires time to be implemented.

These three complementary lines for risk reduction and adaptation to climate change in small tropical islands highlight, first, that site-specific solutions are the appropriate response to site-specific cyclone impacts, and second, that the combination of several solutions (i.e. of relocation/setback and coastal buffer restoration) is required to reduce current and future vulnerability in highly vulnerable (because they are low-lying, physically unstable, and highly-modified) areas.

## **Conclusion**

The study of the impacts on Saint-Martin Island of the most intense series of TCs ever recorded in the Lesser Antilles confirms the major control exerted by high magnitude low frequency climate events on sedimentary coastal systems. These TCs, especially category 5 TC Irma, generated complex and interlinked erosional and accretional processes. Importantly, they caused marked shoreline retreat on most sites, with the minimum NSM value reaching – 166.45 m on the highly-exposed coast of the island, and marked (up to 2 m in height) beach lowering. Seven weeks after the cyclones hit the island, their erosional impacts were still proved, first, by marked erosion scarps cut into upper beaches (0.30 to 0.80 m-high) and sand dunes (up to 4 m high), and second, by the exhumation of the root system of the destroyed indigenous vegetation, where it occurred, over a 5 to 40 m distance, depending on the setting. In areas having little if no vegetation, scour holes and soil scouring were widespread, extending from the upper beach to inland areas over distances ranging from 5 to 20 m. On the most affected beach site, wave attack led to the formation of a 1.20 m-deep and 15 m-long trough extending transversally through the barrier beach. While erosion predominated in beach and upper beach areas, sand accumulation prevailed in inland areas as a result of overwash, where no obstacle, neither natural (i.e. dense vegetation) nor human-built (i.e. buildings and engineered structures), obstructed the sediment transport pathways. Extensive sand sheets (reaching up to 135 m from the inferred ‘pre-cyclone’ vegetation line) indicating significant sediment transfer from the foreshore and beaches to inner land areas were the most common feature observed. At two sites, barrier beach overwashing by the cyclonic waves occurred, which caused sediment deposition in inner lagoons. Importantly, on the highly-exposed, back-reef beaches, the transfer of coral debris to the coast caused the formation of crescent-shaped deposits and of beach ridges at the base of the beach and on the upper beach, respectively, and also led to beach extension along the shoreline. Collectively, these results show that the most

intense TCs, beyond driving important changes in the configuration of beaches and barrier beaches, have constructional impacts on some beach sites.

The analysis of the spatial variability of TCs impacts confirmed the findings of previous studies showing that the cyclone's track, coast exposure and beach configuration drive the nature and intensity of impacts. However, beyond these conclusions, our study emphasizes the crucial role exerted by human-driven changes and interventions, especially vegetation modification and shoreline hardening, on beach response to TCs. While the removal of the indigenous vegetation has exacerbated coastal erosion and marine inundation, shoreline hardening has had contrasting effects. Hardening has reduced shoreline movement and marine inundation, but amplified the detrimental impact of the TCs on the sediment budget of beaches by inhibiting sediment deposition on upper and back beaches while also amplifying beach sediment loss. Based on these findings, we propose a first typology of beach response modes that highlights the site-specific impacts of TCs on small island beaches. The four beach types emphasized in this study include two types of natural beaches, namely back-reef accretional beaches (Type 1) and erosional and migrating barrier beaches (Type 2), and two types of modified beach sites, including back-reef erosional beaches and barrier beaches affected by human disturbances (Type 3) and stable hardened beach sites (Type 4).

Collectively, these findings have major implications for risk reduction and adaptation to climate change in small islands. Highlighting the major role of human-driven feedback effects in exacerbating the vulnerability of coastal areas to future TCs, they show that the reduction of current vulnerability is a key priority to promote adaptation to climate change. This implies (1) the reduction of human asset exposure to climate-related pressures through the relocation of exposed assets and the determination of appropriate set-back lines for future constructions, (2) the protection or restoration of natural buffers, such as beaches and beach-dune systems, through beach nourishment and the revegetation of upper and back-beaches, and (3) the

upgrading of engineered structures in densely-built areas where these structures failed to protect human assets. Importantly, because beach response to TCs is site-specific, solutions should also be adapted to the specificities of each site. Moreover, to optimize benefits, solutions should be combined. For example, combining solutions 1 (relocation) and 2 (coastal buffer restoration) would generate co-benefits for coastal systems (increased resilience) and for the human society (better protection from cyclone-induced devastation). “Building back better” in the post-cyclone reconstruction phase thus appears as a key priority to reduce current and future vulnerability, and thereby promote adaptation to climate change.

### **Acknowledgements**

V.D., V.P. and N.V. were funded by the French CNRS and the French National Research Agency under the STORISK (No.ANR-15-CE03-0003) and TIREX (NoANR-18-OURA-002-03) research projects. Y.K., R.C. and D.B. were funded by the ERDF/C3AF and TIREX (NoANR-18-OURA-002-03) research projects; they warmly thank the main investigators of C3AF, in particular Narcisse Zahibo (University of the French West Indies), Philippe Palany (Météo France), and Frédéric Léone (GRED).

### **References**

- Andrieuff, P., Westercamp, D., Garrabé, F., Bonneton, J.R., Dagain, J., 1988. Stratigraphie de Saint-Martin (Petites Antilles septentrionales). *Géologie de la France* 2-3, 71-88.
- Angelucci, F., Conforti, P., 2010. Risk management and finance along value chains of SIDS. Evidence from the Caribbean and the Pacific. *Food Policy*, 565-575. <http://doi:10.1016/j.foodpol.2010.07.001>
- Battistini, R., Hirschberger, F., 1994. Cordons et lagunes du littoral de Saint-Martin (Antilles Françaises) : dynamique et problèmes d'aménagement. In : Maire, R., Pomel, S., Salomon, J.-N. (Eds.), *Enregistreurs et indicateurs de l'évolution de l'environnement en zone tropicale*. Presses Universitaires de Bordeaux, Bordeaux, pp. 331-344.

- Biribo, N., Woodroffe, C.D., 2013. Historical Area and Shoreline Change of Reef Islands around Tarawa Atoll, Kiribati. *Sustain. Sci.* 8, 345–362. <https://doi.org/10.1007/s11625-013-0210-z>.
- Burningham H., French J., 2017. Understanding coastal change using shoreline trend analysis supported by cluster-based segmentation. *Geomorphology* 282, 131-149. <http://dx.doi.org/10.1016/j.geomorph.2016.09.029>
- Bythell, J.C., Bythell, M., Gladfelter, E.H., 1993. Initial results of long-term coral reef monitoring program: impacts of hurricane Hugo at Buck Island Reef National Monument, St. Croix, U.S. Virgin Islands. *J Exp Mar Biol Ecol* 172, 171-183. [http://doi:10.1016/0022-0981\(93\)90096-7](http://doi:10.1016/0022-0981(93)90096-7)
- Cahoon, D.R., Hensel, P., Rybczyk, J., McKee, K.L., Proffitt, E., Perez, B.C., 2003. Mass tree mortality leads to mangrove peat collapse at Bay Islands, Honduras after Hurricane Mitch, *J Ecol* 91, 1093-1105. <http://doi: 10.1046/j.1365-2745.2003.00841.x>
- Cambers, G., 1997. Beach changes in the Eastern Caribbean islands: hurricane impacts and implications for climate change. *J Coast Res SI* 24, 29-47.
- Cambers, G., 2009. Caribbean beach changes and climate change adaptation. *Aquatic Ecosystem Health and Management* 12(2), 168-176. <http://dx.doi.org/10.1080/14634980902907987>
- Caron, V., 2011. Contrasted textural and taphonomic properties of high-energy wave deposits cemented in beachrocks (St. Bartholomew Island, French West Indies). *Sediment Geol*, 189-208. <http://doi:10.1016/j.sedgeo.2011.03.002>
- Cécé, R., Bernard, D., d’Alexis, C., Dorville, J., 2014. Numerical Simulations of Island-Induced Circulations and Windward Katabatic Flow over the Guadeloupe Archipelago. *Mon. Wea. Rev.* 142, 850–867. <https://doi.org/10.1175/MWR-D->



Chauvet, M., Bodéré, G., Mompelat, J.-M., Oliveros, C., Bozorgan, A., 2007. Caractérisation des impacts de la houle sur les rivages de la Guadeloupe au passage de l'ouragan Dean (août 2007). Rapport BRGM/RP-55911-FR (14 pp.).

Chauvet, M., Joseph, B., 2008. Caractérisation des impacts de la houle liée à l'ouragan Omar sur la côte sous le vent de la Guadeloupe (octobre 2008). Rapport BRGM/RP-56869-FR (130 pp.).

Cooper, J.A.G., Jackson, D.W.T., Gore, S., 2013. A groundswell event on the coast of the British Virgin Islands: spatial variability in morphological impact. *J. Coast. Res.* SI 65, 696-701. <https://dx.doi.org/10.2112/SI65-118.1>

Cooper, J.A.G., McKenna, J., 2008. Working with natural processes: the challenge for coastal protection strategies. *Geogr J* 174(4), 315–331. <http://dx.doi.org/10.1111/j.1475-4959.2008.00302.x>

Cooper, J.A.G., Pile, J., 2014. The adaptation-resistance spectrum: a classification of contemporary adaptation approaches to climate-related coastal change. *Ocean Coast Manage* 94, 90–98. <http://dx.doi.org/10.1016/j.ocecoaman.2013.09.006>

Crabbe, M.J., Martinez, E., Garcia, C., Chub, J., Castro, L., Guy, J., 2008. Growth modelling indicates hurricanes and severe storms are linked to low recruitment in the Caribbean. *Mar Environ Res* 65, 364-368. <http://doi:10.1016/j.marenvres.2007.11.006>

DDE Guadeloupe, Service Aménagement et Urbanisme, 2008. Mise à jour du plan de prévention des risques naturels de la collectivité territoriale de Saint-Martin : note méthodologique. Rapport GTR/DDEG/0508-484-AV2 (96 pp.).

Degrace, J. N., 2017. Passage de l'ouragan exceptionnel Irma sur les îles françaises des Antilles les 05 et 06 septembre 2017. Communiqué de presse, 12/09/2017, Direction Inter-régionale Antilles-Guyane, Météo-France (6 pp.).

De Scally, F.A., 2008. Historical tropical cyclone activity and impacts in the Cook Islands. *Pac Sci* 62(4), 443-459. [http://dx.doi.org/10.2984/1534-6188\(2008\)62\[443:HTCAAI\]2.0.CO;2](http://dx.doi.org/10.2984/1534-6188(2008)62[443:HTCAAI]2.0.CO;2)

De Scally, F.A., 2014. Evaluation of storm surge risk: a case study from Rarotonga, Cook Islands. *International Journal of Disaster Risk Reduction* 7: 9-27.

<http://dx.doi.org/10.1016/j.ijdrr.2013.12.002>

Dorville, J.-F., Zahibo, N., 2010. Hurricane Omar waves impact on the west coast of the Guadeloupe Island, October 2008. *The Open Oceanography Journal* 4, 83-91.

Duvat, V., 2008. Le système du risque à Saint-Martin (Petites Antilles françaises).

*Développement Durable et Territoires* 11. <http://dx.doi.org/10.4000/developpementdurable.7303>

Duvat, V., 2013. Coastal protection structures in Tarawa Atoll, Republic of Kiribati. *Sustain. Sci.* 8, 363–370. <http://dx.doi.org/10.1007/s11625-013-0205-9>

Duvat, V., Magnan, A., 2014. Le cyclone Luis à Saint-Martin. In: *Des catastrophes... “naturelles” ? Le Pommier*, Coll. Essais, Paris, pp. 123-147.

Duvat, V., Magnan, A., Etienne, S., Salmon, C., Pignon-Mussaud, C., 2016. Assessing the impacts of and resilience to Tropical Cyclone Bejisa, Reunion Island (Indian Ocean). *Natural Hazards* 83, 601-640. <http://doi:10.1007/s11069-016-2338-5>

Duvat, V., Pillet, V., 2017. Shoreline changes in reef islands of the Central Pacific: Takapoto Atoll, Northern Tuamotu, French Polynesia. *Geomorphology* 282, 96–118. <https://doi.org/10.1016/j.geomorph.2017.01.002>.

Duvat, V.K.E., Volto, N., Salmon, C., 2017a. Impacts of category 5 tropical cyclone Fantala (April 2016) on Farquhar Atoll, Seychelles Islands. *Geomorphology* 298, 41-62. <http://doi:10.1016/j.geomorph.2017.09.022>

Duvat, V.K.E., Salvat, B., Salmon, C., 2017b. Drivers of shoreline change in atoll reef islands of the Tuamotu Archipelago. French Polynesia. *Global and Planetary Change* 158, 134-154. <https://doi.org/10.1016/j.gloplacha.2017.09.016>

- Etienne, S., 2012. Marine inundation hazards in French Polynesia: geomorphic impacts of Tropical Cyclone Oli in February 2010. *Geol Soc SP v. 361*, 21-39. <http://doi: 10.1144/SP361.4>
- Etienne S., Terry J.P., 2012. Coral boulders, gravel tongues and sand sheets: Features of coastal accretion and sediment nourishment by Cyclone Tomas (March 2010) on Taveuni Island, Fiji. *Geomorphology* 175–176, 54–65. <http://dx.doi.org/10.1016/j.geomorph.2012.06.018>
- Ferdinand, I., O'Brien, G., O'Keefe, P., Jayawickrama, J., 2012. The double blind of poverty and community disaster risk reduction: a case study from the Caribbean. *International Journal of Disaster Risk Reduction* 2, 84-94. <http://dx.doi.org/10.1016/j.ijdrr.2012.09.003>
- Fletcher, C.H, Bochicchio, C., Conger, C., Engels, M., Feirstein, F., Frazer, N., Glenn, C., Grigg, R.W., Grossman, E.E., Harvey, J.N., 2008. Geology of Hawaii reefs. In: Riegl, BM and RE Dodge (eds.), *Coral Reefs of the World, Vol. 1*. Springer Science, Dordrecht, Netherlands, pp. 435-487.
- Ford, M.R., Kench, P.S., 2014. Formation and adjustment of typhoon-impacted reef islands interpreted from remote imagery: Nadikdik Atoll, Marshall Islands. *Geomorphology* 214, 216–222. <https://doi.org/10.1016/j.geomorph.2014.02.006>.
- Hapke, C.J., Kratzmann, M.G., Himmelstoss, E.A., 2013. Geomorphic and human influence on large-scale coastal change. *Geomorphology* 199, 160–170. <http://dx.doi.org/10.1016/j.geomorph.2012.11.025>
- Hubbard, D.K., Parsons, K.M., Bythell, J.C., Walker, N.D., 1991. The effects of hurricane Hugo on the reefs and associated environments of St. Croix, US Virgin Islands: a preliminary assessment. *J Coastal Res* 3, 33-48. [http://dx.doi.org/10.1007/978-90-481-2639-2\\_135](http://dx.doi.org/10.1007/978-90-481-2639-2_135)
- INSEE, 2013. Saint-Martin : terre d'accueil et de contrastes, *Insee Analyses* 24, Juin 2017 (4 pp.).
- Krien, Y., Testut, L., Islam, A.S., Bertin, X., Durand, F., Mayet, C., Tazkia, A.R., Becker, M., Calmant, S., Papa, F., Ballu, V., Shum, C.K., Khan, Z.H., 2017. Towards improved storm surge

models in the northern Bay of Bengal. *Cont Shelf Res* 135, 58-73.

<http://dx.doi.org/10.1016/j.csr.2017.01.014>. 9.

Imbert, D., Portecop, J., 2008. Hurricane disturbance and forest resilience: Assessing structural vs. functional changes in a Caribbean dry forest. *Forest Ecology and Management* 255, 3494–3501. <http://doi:10.1016/j.foreco.2008.02.030>

Mahabot, M.-M., Pennober, G., Suanez, S., Troadec, R., Delacourt., C., 2017. Effect of Tropical Cyclones on Short-Term Evolution of Carbonate Sandy Beaches on Reunion Island, Indian Ocean. *J Coast Res* 33 (4), 839-853. <http://dx.doi.org/10.2112/JCOASTRES-D-16-00031.1>

Mallela, J., Crabbe, M.J.C., 2009. Hurricanes and coral bleaching linked changes in coral recruitment in Tobago. *Mar Environ Res* 68, 158-162.

<http://dx.doi.org/10.1016/j.marenvres.2009.06.001>

Mann, T., Westphal, H., 2014. Assessing long-term changes in the beach width of reef islands based on temporally fragmented remote sensing data. *Remote Sens.* 6, 6961–6987.

<https://doi.org/10.3390/rs6086961>

Martin, R., Mompellat, J.-M., 2000. Les conséquences de la houle générée par le cyclone Lenny sur la côte sous le vent de la Guadeloupe. Rapport BRGM/RP-50169-FR (35 pp.).

McIntyre W.G., Walker H.J., 1964. Tropical cyclones and coastal morphology in Mauritius. *Ann Am Assoc Geogr.* 54 (4), 582-596. <https://doi.org/10.1111/j.1467-8306.1964.tb01786.x>

Météo-France, 2005. Atlas Climatique : l'environnement atmosphérique de la Guadeloupe, Saint-Barthélemy et Saint-Martin. Météo-France Antilles-Guyane (92 pp.).

Monnier, Y., 1987. Aménagements touristiques et bouleversements écologiques dans les petites îles : l'exemple de Saint-Martin. In : Doumenge, J.-P., Perrin, M.-F., Benoist, J.-P.,

Singaravelou, Huetz De Lempis, C., *Iles tropicales : insularité, insularisme*. Congress

Proceedings, 23-25 October 1986, Collections Iles et Archipels, n°8, CRET, Bordeaux, pp. 17-33.

Mycoo, M.A., 2017. Beyond 1.5°C: vulnerabilities and adaptation strategies for Caribbean Small Island Developing States. *Reg Environ Change*. <https://doi.org/10.1007/s10113-017-1248-8>

Nunn, P.D., 2009. Responding to the challenges of climate change in the Pacific Islands: management and technological perspectives. *Clim Res* 40, 211-231. <http://dx.doi.org/10.1007/s10584-016-1646-9>

Nurse, L.A., McLean, R.F., Agard, J., Briguglio, L.P., Duvat-Magnan, V., Pelesikoti, N., Tompkins, E., Webb, A., 2014. Small islands. In: Barros, V.R., Field, C.B., Dokken, D.J., Mastrandrea, M.D., Mach, K.J., Bili, T.E., Chatterjee, M., Ebi, K.L., Estrada, Y.O., Genova, R.C., Girma, B., Kissel, E.S., Levy, A.N., MacCracken, S., Mastrandrea, P.R., White, L.L. (Eds.), *Climate Change 2014: Impacts, Adaptation and Vulnerability. Part B: Regional Aspects. Contribution of Working Group II to the Fifth Assessment Report of the Intergovernmental Panel on Climate Change*. Cambridge University Press, Cambridge and New York, pp. 1613–1654.

OECS Grenada, 2004. Macro-Socio-Economic Assessment of the Damages Caused by Hurricane Ivan, September 7<sup>th</sup> 2004. Organisation of East Caribbean States (OECS), OECS Secretariat, Castries, St. Lucia (126 pp.).

Park, L.E., Siewers, F.D., Metzger, T., Sipahioglu, S., 2009. After the hurricane hits: recovery and response to large storm events in a saline lake, San Salvador Island, Bahamas. *Quaternary International* 195, 98-105. <https://doi.org/10.1016/j.quaint.2008.06.010>

Perry, C.T., Smithers, S.G., Kench, P.S., Pears, B., 2014. Impacts of Cyclone Yasi on nearshore terrigenous sediment-dominated reefs of the central Great Barrier Reef, Australia. *Geomorphology* 222, 92-105. <http://dx.doi.org/10.1016/j.geomorph.2014.03.012>

- Ramalho, R., 1971. Carte géomorphologique de l'île de Saint-Martin (Guadeloupe). Étude de photo-interprétation.
- Rey, T., Le De, L., Léone, F., David, G., 2017. An integrative approach to understand vulnerability and resilience post-disaster. The 2015 cyclone Pam in urban Vanuatu as case study. *Disaster Prevention and Management: An International Journal* 26(3), 259-275.  
<https://doi.org/10.1108/DPM-07-2016-0137>
- Richmond, N., Sovacool, B.K., 2012. Bolstering resilience in the coconut kingdom: improving adaptive capacity to climate change in Vanuatu. *Energy Policy* 50, 843-848.  
<http://doi:10.1016/j.enpol.2012.08.018>
- Scheffers, A., Scheffers, S., 2006. Documentation of the impact of Hurricane Ivan on the coastline of Bonaire (Netherlands Antilles). *J Coastal Res* 22, 1437-1450.  
<http://dx.doi.org/10.2112/05-0535.1>
- Scoffin, T.P., 1993. The geological effects of hurricanes on coral reefs and interpretation of storm deposits. *Coral Reefs* 12, 203-221. <https://doi.org/10.1007/BF00334480>
- Scopélitis, J., Andréfouët, S., Phinn, S., Chabanet, P., Naim, O., Tourrand, C., Done, T., 2009. Changes of coral communities over 35 years: integrating in situ and remote-sensing data on Saint-Leu reef (la Réunion, Indian Ocean). *Estuar Coast Shelf S* 84, 342-352.  
<http://dx.doi.org/10.1016/j.ecss.2009.04.030>
- Skamarock, W.C., Klemp, J.B., Dudhia, J., Gill, D.O., Barker, D.M., Duda, M.G., Huang, X.-Y., Wang, W., Powers, J.G., 2008. A description of the Advanced Research WRF version 3. Tech. Rep. NCAR/TN-475+STR, National Center for Atmospheric Research, 125 pp.  
[Available online at [http://www.mmm.ucar.edu/wrf/users/docs/arw\\_v3.pdf](http://www.mmm.ucar.edu/wrf/users/docs/arw_v3.pdf).]
- Solomiac, H., 1974. Carte géologique de Saint-Martin.
- Stoddart, D. R., 1963. Effects of hurricane Hattie on the British Honduras reefs and cays, October 30-31, 1961, *Atoll Res Bull* 95, 1-142.

- Stoddart, D. R., 1965. Re-survey of hurricane effects on the British Honduras reefs and cays, *Nature* CCVII, 589-592.
- Stoddart D.R., 1971. Coral Reefs and Islands and Catastrophic Storms. In: J. A. Steers (ed.), *Applied Coastal Geomorphology*. Palgrave Macmillan, pp. 155-197.
- Strobl, E., 2012. The economic growth impact of natural disasters in developing countries: evidence from hurricane strikes in the Central American and Caribbean regions. *J Dev Econ* 97, 130-141. <http://dx.doi.org/10.1016/j.jdeveco.2010.12.002>
- Terry, J.P., Garimella, S., Kostaschuk, R.A., 2002. Rates of floodplain accretion in a tropical island river system impacted by cyclones and large floods. *Geomorphology* 42, 171-182. <http://dx.doi.org/10.1016/S0169-555X%2801%2900084-8>
- Terry, J.P., Falkland, A.C., 2010. Responses of atoll freshwater lenses to storm-surge overwash in the Northern Cook Islands, *Hydrogeology Journal*, 18(3), 749-759. <http://dx.doi.org/10.1007/s10040-009-0544-x>
- Thieler, E.R., Himmelstoss, E.A., Zichichi, J.L., Ergul, A., 2009. The Digital Shoreline Analysis System (DSAS) Version 4.0: an ArcGIS extension for calculating shoreline change. USGS Open File Report 2008-1278, pp. 1–79.
- Westercamp, D., Tazieff, H., 1980. Martinique, Guadeloupe, Saint-Martin, La Désirade. *Guides géologiques régionaux*, Masson, Paris, (135 pp.).
- Yates, M.L., Le Cozannet, G., Garcin, M., Salai, E., Walker, P., 2013. Multi-decadal atoll shoreline change on Manihi and Manuae, French Polynesia. *J Coast Res* 29, 870–892. <http://dx.doi.org/10.2112/JCOASTRES-D-12-00129.1>
- Zhang, Y., Ye, F., Stanev, E.V., Grashorn, S., 2016. Seamless cross-scale modeling with SCHISM. *Ocean Model* 102, 64–81. <http://dx.doi.org/10.1016/j.ocemod.2016.05.002>

### Figure captions

Fig 1. Location map of Saint-Martin Island in the Lesser Antilles.

Fig 2. Main characteristics of Saint-Martin Island.

Fig 3. Characteristics of tropical cyclones Irma, José and Maria (September 2017) in the vicinity of Saint-Martin Island.

a Track and intensities of Irma, José and Maria given by the NHC's advisories. The black rectangle shows the study area. The colours depict the cyclone category along the track (red, yellow and green for category 5, 4, and 3, respectively). Times are given in UTC. b Maximum 10 mn-sustained winds at 10 m in the Lesser Antilles, estimated by merging CFSR data with empirical laws for Irma (left) and José (right). c Maximum surface winds for Irma at Saint-Martin, estimated by the atmospheric model WRF at 0.4 km resolution. d Maximum significant wave heights (in metres) and corresponding mean wave directions (vectors) for Irma (left) and José (right) at Saint-Martin using the wave-current coupled model SCHISM-WWM (e.g. Zhang et al., 2016; Krien et al., 2017), with a timestep of 5 mn and a maximum resolution of 100 m. The bathymetry was obtained by digitizing navigational charts provided by the SHOM (Service Hydrographique et Océanographique de la Marine).

Fig 4. Shoreline indicators used in this study.

a Digitization of the pre-cyclone position of the stability line in natural (i.e. unbuilt) areas, where it corresponds to the vegetation line (here, at Grandes Cayes Beach). b Inferred pre-cyclone position of the stability line in built-up areas (here, in Marigot Bay), where it corresponds to the seaward limit of engineered structures and buildings. c Digitization of the base of the beach on pre-cyclone images (here, at Petites Cayes Beach). d Digitization of the pre- and post-cyclone stability line and the inner limit of cyclone-driven sediment deposits (Grandes Cayes Beach). e Digitization of the base of the beach on post-cyclone images (Petites Cayes Beach). Of note, the comparison of a-d and of c-e shows the highly destructive impacts of the cyclones on the coastal vegetation.

Fig 5. Spatial extent of digitized shorelines.

Data generation was constrained by cloud cover, hydrodynamics and turbidity at some locations.

Fig 6. Inferred impacts of September 2017 tropical cyclones on shoreline position.

This figure highlights first, the contrasting response of the stability line depending on coast exposure, and second, the contrasting behaviours of the stability line and of the base of the beach, as the former predominantly exhibited retreat while the latter mainly experienced either stability or advance.

Fig 7. Variations observed in the response of the stability line to September 2017 tropical cyclones on Saint-Martin Island.

For beach site numbering, see Fig 6. The line in bold represents the variability of the NSM (Net Shoreline Movement) values obtained for each beach site depending on its exposure, based on the generation of 10 m-interval transects along the shoreline. While some beach sites, especially along the highly exposed eastern coast of the island, experienced highly contrasting NSM values along their shoreline (e.g. sites 4, 16 and 25), other sites exhibited more homogenous NSM values (e.g. 1, 2, 15, 19, 21-24, 27, 29). Within-site variability shows limited correlation with site exposure.

Fig 8. Inferred erosional impacts of September 2017 tropical cyclones on Saint-Martin Island.

a Exhumed beachrock slabs indicating beach erosion at Longue Bay. The red arrow shows the 5 m-wide inner part of beachrock slabs that was exhumed by the cyclonic waves. b Marked beach lowering indicated by the exhumation of the previously buried lower part of the retaining wall of a seaside property at Red Bay. Note the total destruction of the vegetation in front of the wall and the dismantling of ripraps resulting from wave impact. c Cyclone-driven sand dune retreat revealing underlying soil formation,



which has also been eroded by the cyclonic waves. d and e Cyclone-generated transversal trenches extending from the upper beach to the inner land area at Orient Bay North (25 m long) and Embouchure Bay (10 m long), respectively. e Also shows vegetation uprooting and destruction over a distance of around 20 m from the vegetation line. f The red arrow shows marked soil scouring over a distance of 20 m at the southern end of Guana Bay. Before the cyclone, this area was entirely covered by dense vegetation.

Fig 9. Inferred accretional impacts of the September 2017 tropical cyclones on Saint-Martin Island.

a Cyclone-generated 2 to 8 cm-thick sand sheets extending over a maximum distance of 75 m from the pre-cyclone vegetation line, central part of Mullet Bay. b 0.80 m-thick sand deposits recorded in open areas between buildings at Guana Bay. c and d Gibb's Bay. c Sediment deposition resulting from wave overwashing of the 40-50 m-wide barrier beach. Sand lobes formed along the entire lagoon-side shoreline. d Sand deposition against the natural vegetation in the inner part of the barrier beach. e, f and g show accretional features observed on Petites Cayes Beach. e The beach ridge that formed at the top of the shrubby vegetation, as a result of the transfer of coral debris and blocks from the fringing reef to the beach. f Major role of the dense coastal vegetation in trapping coral debris and blocks. g Crescent-shaped shingle deposit structure that formed at the base of the beach. h Beachrock fragments' accumulation against cyclone-generated erosion scarps cut in Longue Bay sand dunes. These deposits result from the dismantling of exhumed beachrock slabs that can be seen in the wave breaking zone on the same photograph.

Fig 10. Impacts of coastal development on beach response.

See Fig 6 for the legend of maps.

a to d Impacts of longitudinal constructions on shoreline response and on cyclone-driven erosional and accretional processes. On a (Marigot Bay) and b (Longue Bay), as a result of the construction of massive engineered structures (here, rip-raps), the stability line exhibited positional stability. On c and d (Red Bay) rip-raps, which were constructed by seaside residents, were partially dismantled by the cyclonic waves. As a result, wave reflection on the frontage of houses caused marked beach lowering ( $-0.80$  to  $-1.60$  m on c, and  $-1.50$  to  $-2$  m on d), exhuming buildings foundations. On e (Guana Bay) seaside houses were either wiped out by the cyclonic waves (on the foreground), or severely damaged (on the background). Here too, wave reflection caused marked beach lowering (up to  $-2$  m in front of buildings). f (southern end of Orient Bay) illustrates widespread sand deposition in cleared areas. Here, at a distance of 60 m from the pre-cyclone stability line, sand deposits reached 0.80 m in thickness. g Piles of sand resulting from the removal of cyclonic deposits (around  $300\text{ m}^3$ ) both inside and in front of seaside properties along the 100 m-long urbanized shoreline section of Lucas Bay.

Fig 11. Beach type 1: back-reef accretional beach (e.g. Petites Cayes Beach).

Noteworthy are the marked retreat of the vegetation line and the marked advance of the base of the beach. The latter, which was caused by a massive transfer of coral shingle and rubble, including corals broken by the cyclonic waves, to the coast, led to the formation of a new beach (left side of the image). Sediment inputs also took the shape of extensive sand sheets.

Fig. 12. Beach type 2: erosional and migrating barrier beach (e.g. Gibb's Bay).

The combination of stability (i.e. vegetation) line retreat and of massive beach-to-lagoon sand transfer caused, first, the landward migration of the barrier beach, and second, the partial infilling of the lagoon.

Fig 13. Beach type 3: back-reef erosional beach or barrier beach affected by human disturbances (e.g. Orient Bay)

The inner limit of cyclone-driven sediment deposits was not detectable in the central part of the bay, due to post-cyclone human intervention. The erosional impacts of the cyclones were aggravated by coastal development, especially the removal of the natural vegetation, which exacerbated wave penetration, beach erosion and soil scouring.

Fig 14. Beach type 4: stable hardened beach sites (e.g. Simpson Bay).

a and b illustrate the case of highly-modified barrier beaches, either urbanized or having major infrastructures (here, Simpson Bay's international airport). The resistance of seaside buildings and engineered structures (mainly ripraps) which fix the shoreline explains first, the positional stability of the shoreline, and second, limited sediment deposition in inner land areas (with the exception of the runway).

Table 1. Main characteristics of Saint-Martin Island beaches (source: satellite image analysis and October-November 2017 fieldwork)

\*\* indicates sites where a significant part of the lagoon (>30%) has been reclaimed since 1947. \*\*\* indicates sites having a small swamp.

Lagoons have either a longitudinal, or a transversal orientation in relation to the shoreline. Some sites already had a limited vegetation cover in 1947, as a result of either clearing, or limited development due to drought. 'Natural' applies to beaches that exhibit limited if no human-induced disruption of their natural dynamics. Moderately disturbed applies to beaches showing human-induced disturbances that partly affect their behaviour (e.g. vegetation clearing affecting transversal sediment transport and deposition, scattering buildings interacting with waves). Highly disturbed applies to beaches having highly modified dynamics as a result of human activities (e.g. densely urbanized sites, where the natural vegetation was entirely removed; armoured sites).

Table 2. Main features of the tropical cyclones of September 2017.

Table 3. Characteristics of satellite images used in this study.

Table 4. Change in the position of the stability line from 12 February 2017 (7 months before the cyclones) to 10-14 September 2017 (post-cyclone situation). Of note, there were no accretional transects.

Table 5. Change in the position of the base of the beach from 12 February 2017 (7 months before the cyclones) to 14 September 2017 (post-cyclone situation).

SM1. Time series of significant wave heights (blue) and mean wave directions (red, nautical convention) given by the Ifremer global wave model at two points located in the vicinity of Saint Martin.

SM2. Erosional features observed after the passage of tropical cyclones Irma and Jose on Saint-Martin Island SM2 (source: comparative analysis of the pre- and post-cyclone satellite images of 12 February 2017 and 10 and 14 September 2017, and fieldwork conducted in October-November 2017).

\* Based on average NSM values. \*\* Based on the % of transects indicating shoreline retreat. \*\*\* Two trenches have been dug between 11 and 14 September 2017 to allow the discharge of the lagoon to the sea. These trenches were therefore not cyclone-generated.

SM3. Accretional features observed after the passage of tropical cyclones Irma and Jose on Saint-Martin Island (source: comparative analysis of the satellite images of 12 February 2017 and 10 and 14 September 2017, and fieldwork conducted in October-November 2017).

Beach name and type Barrier beach (BB) Beach system backed onto inner relief (B)	Physical features				Anthropogenic features			
	Reef type	Offshore islet(s)	Beachrock slabs	Vegetation type	Coastal urbanization or seaside developments	Tracks or breaches through the beach system	Extensive vegetation clearing (C) or removal (R)	S an o pro
1. Petites Cayes Bay (B)	/	No	No	Mixed	No	Yes	No	
2. Petites Cayes Beach (B)	Embryonic	No	Yes	Mixed	No	Yes	No	
3. Grandes Cayes Beach (B)	Fringing	Yes	No	Indigenous	Yes	Yes	No	
4. Cul de Sac Bay** (BB)	Barrier	Yes	No	Mixed	Yes	Yes	Yes (R)	
5. Orient Bay North (BB)	/	Yes	No	Mixed	Yes	Yes	Yes (C)	
6. Orient Bay Central and South (BB)	Fringing	Yes	No	Introduced	Yes	Yes	Yes (R)	
7. Embouchure Bay (BB)	Fringing	Yes	No	Mixed	No	Yes	No	
8. Lucas Bay*** (B)	Fringing	No	Yes	Mixed	Yes	Yes	Yes (C)	
9. Dawn Beach (B)	Fringing	No	No	Introduced	Yes	Yes	Yes (R)	
10. Gibb's Bay (BB)	/	No	No	Indigenous	No	Yes	No	
11. Guana Bay*** (B)	/	No	No	Mixed	Yes	Yes	Yes (C)	
12. Great Bay (BB)	/	No	No	Introduced	Yes	Yes	Yes (R)	
13. Little Bay (BB)	/	No	n.d.	Mixed	Yes	Yes	Yes (R)	
14. Cay Bay*** (B)	/	No	n.d.	n.d.	Yes	Yes	Yes (C)	
15. Cole Bay (BB)	/	No	Yes	n.d.	Yes	Yes	Yes (R)	
16. Simpson Bay (BB)	/	No	Yes	Mixed	Yes	Yes	Yes (R)	
17. Maho Bay*** (B)	/	No	Yes	Introduced	Yes	Yes	Yes (R)	
18. Mullet Beach (BB)	/	No	Yes	Mixed	No	Yes	Yes (R)	
19. Longue Bay (BB)	/	No	Yes	Mixed	Yes	Yes	Yes (C)	
20. Plum Bay (B)	/	No	Yes	Mixed	Yes	Yes	Yes (C)	
21. Red Bay** (BB)	/	No	Yes	Mixed	Yes	Yes	Yes (C)	
22. Cayes Bay (B)	/	Yes	n.d.	n.d.	No	Yes	No	
23. Small Bay (B)	/	Yes	n.d.	n.d.	No	No	No	
24. Anse des Sables (B)	/	No	n.d.	n.d.	No	Yes	No	
25. Nettle Bay (BB)	/	No	Yes	Indigenous (W) + introduced (E)	Yes	Yes	Yes (R)	
26. Marigot Bay (BB)	/	No	Yes	Mixed	Yes	Yes	Yes (R)	
27. La Potence Bay** (BB)	/	No	Yes	/	Yes	Yes	Yes (R)	
28. Anse des Pères*** (BB)	/	No	n.d.	/	No	Yes	Yes (R)	
29. Friar's Bay (BB)	/	No	Yes	Introduced	No	Yes	Yes (R)	
30. Anse Heureuse** (BB)	/	No	Yes	Mixed	No	Yes	No	
31. Grand Case Bay** (BB)	/	No	Yes	Introduced	Yes	Yes	Yes (R)	
32. Bell Hill Beach (B)	/	Yes	n.d.	n.d.	No	No	No	
33. Anse Marcel (BB)	/	Yes	No	Introduced	Yes	Yes	Yes (R)	

Table 1. Main characteristics of Saint-Martin Island beaches (source: satellite image analysis and October-November 2017 fieldwork)

\*\* indicates sites where a significant part of the lagoon (>30%) has been reclaimed since 1947. \*\*\* indicates sites having a small swamp.

Lagoons have either a longitudinal, or a transversal orientation in relation to the shoreline. Some sites already had a limited vegetation cover in 1947, as a result of either clearing, or limited development due to drought. 'Natural' applies to beaches that exhibit limited if no human-induced disruption of their natural dynamics. Moderately disturbed applies to beaches showing human-induced disturbances that partly affect their behaviour (e.g. vegetation clearing affecting transversal sediment transport and deposition, scattering buildings interacting with waves). Highly disturbed applies to beaches having highly modified dynamics as a result of human activities (e.g. densely urbanized sites, where the natural vegetation was entirely removed; armoured sites).

	Irma	José	Maria
Sustained wind (km/h)	296	250	278
Wind gusts (km/h)	361	296	343
Pressure (hPa)	914	938	909
Distance from Saint-Martin (km)	0	130	170

Table 2. Main features of the tropical cyclones of September 2017.

Date	Provider	Sensor	Image type	Pixel size (m)	Site concerned
January-March 2013	IGN (National Geographical Institute)	/	Ortho-photography	0.5	/
12 February 2017	Airbus Defence & Space	Pléiades-1B	Panchromatic	0.5	All
10 September 2017	Airbus Defence & Space	Pléiades-1B	Panchromatic	0.5	1, 3, 4, 5, 6, 7, 8, 9, 10, 11, 12, 16, 21, 25 (W & E), 26 (W), 28 (E), 32, 33
14 September 2017	Airbus Defence & Space	Pléiades-1A	Panchromatic	0.5	2, 15, 17, 18, 19, 20, 22, 23, 24, 25 (centre), 26 (E), 27, 28 (W), 29, 30

Table 3. Characteristics of satellite images used in this study.

Location	Beach name	Number of transects	NSM (m)			Stable transects		Erosional transects	
			Average	Min	Max	Nb	%	Nb	%
North	1. Petites Cayes Bay	17	-18.84	-28.95	-8.30	0	0.00	17	100.00
	2. Petites Cayes Beach	44	-26.52	-42.80	-10.86	0	0.00	44	100.00
	21. Red Bay	142	-5.13	-15.65	0.00	41	28.87	101	71.13
	22. Cayes Bay	35	-9.11	-27.24	-2.58	0	0.00	35	100.00
	23. Small Bay	11	-9.96	-22.12	-2.50	0	0.00	11	100.00
	24. Anse des Sables	28	-1.20	-4.46	0.00	20	71.43	8	28.57
	25. Nettle Bay	246	-21.60	-108.22	0.00	62	25.20	184	74.80
	26. Marigot Bay	131	-2.41	-41.60	0.00	110	83.97	21	16.03
	27. La Potence Bay	105	-0.95	-12.07	0.00	93	88.57	12	11.43
	28. Anse des Pères	69	-8.95	-45.58	0.00	24	34.78	45	65.22
	29. Friar's Bay	25	-7.30	-17.31	-0.67	4	16.00	21	84.00
	30. Anse Heureuse	29	-9.83	-34.50	0.00	1	3.45	28	96.55
	31. Grand Case Bay	n.d.	n.d.	n.d.	n.d.	n.d.	n.d.	n.d.	n.d.
32. Bell Hill Beach	11	-32.73	-67.53	-6.67	0	0.00	11	100.00	
33. Anse Marcel	42	-14.37	-64.17	0.00	3	7.14	39	92.86	
East	3. Grandes Cayes Beach	103	-34.55	-70.04	-0.85	5	4.85	98	95.15
	4. Cul de Sac Bay	62	-51.64	-166.45	-0.65	1	1.61	61	98.39
	5. Orient Bay North	51	-36.80	-102.82	0.00	3	5.88	48	94.12
	6. Orient Bay Central and South	139	-68.28	-134.68	-5.13	0	0.00	139	100.00
	7. Embouchure Bay	163	-36.04	-87.00	0.00	13	7.97	150	92.03
	8. Lucas Bay	54	-28.71	-65.74	0.00	5	9.26	49	90.74
	9. Dawn Beach	58	-9.84	-29.50	-0.07	6	10.34	52	89.66
	10. Gibb's Bay	15	-22.06	-34.42	-6.67	0	0.00	15	100.00
11. Guana Bay	41	-38.68	-65.29	-21.02	0	0.00	41	100.00	
South	12. Great Bay	154	-7.82	-49.99	0.00	77	50.00	77	50.00
	13. Little Bay	n.d.	n.d.	n.d.	n.d.	n.d.	n.d.	n.d.	n.d.
	14. Cay Bay	n.d.	n.d.	n.d.	n.d.	n.d.	n.d.	n.d.	n.d.
	15. Cole Bay	107	-2.29	-7.91	0.00	59	55.14	48	44.86
	16. Simpson Bay	253	-12.74	-99.79	0.00	75	29.64	178	70.36
	17. Maho Bay	30	-9.63	-44.15	0.00	20	66.67	10	33.33
	18. Mullet Beach	47	-6.06	-32.46	0.00	13	27.66	34	72.34
West	19. Longue Bay	170	-1.94	-12.25	0.00	112	65.88	58	34.12
	20. Plum Bay	120	-3.92	-30.18	0.00	71	59.17	49	40.83

Table 4. Change in the position of the stability line from 12 February 2017 (7 months before the cyclones) to 14 September 2017 (post-cyclone situation). Of note, there were no accretional transects.

Beach name	Number of transects	NSM (m)			Accretional transects		Stable transects		Erosional transects	
		Average	Min	Max	Nb	%	Nb	%	Nb	%
1. Petites Cayes Bay	19	1.32	-4.06	4.63	4	21.05	13	68.42	2	10.53
2. Petites Cayes Beach	99	8.26	-4.18	21.44	72	72.73	25	25.25	2	2.02
3. Grandes Cayes Beach	98	3.14	-4.20	9.80	58	59.19	35	35.71	5	5.10
7. Embouchure Bay	170	1.24	-4.42	9.64	41	24.12	121	71.18	8	4.70

Table 5. Change in the position of the base of the beach from 12 February 2017 (7 months before the cyclones) to 14 September 2017 (post-cyclone situation).

ACCEPTED MANUSCRIPT

## Highlights

- September 2017 cyclones caused a shoreline retreat reaching up to 165 m
- Upper beaches and back-beaches generally exhibited post-cyclone sediment deposition
- Vegetation modification increased storm-induced flooding and decreased beach ridge development
- Shoreline hardening aggravated cyclone-induced sediment loss
- Relocation and set-back lines would allow reducing current and future vulnerability



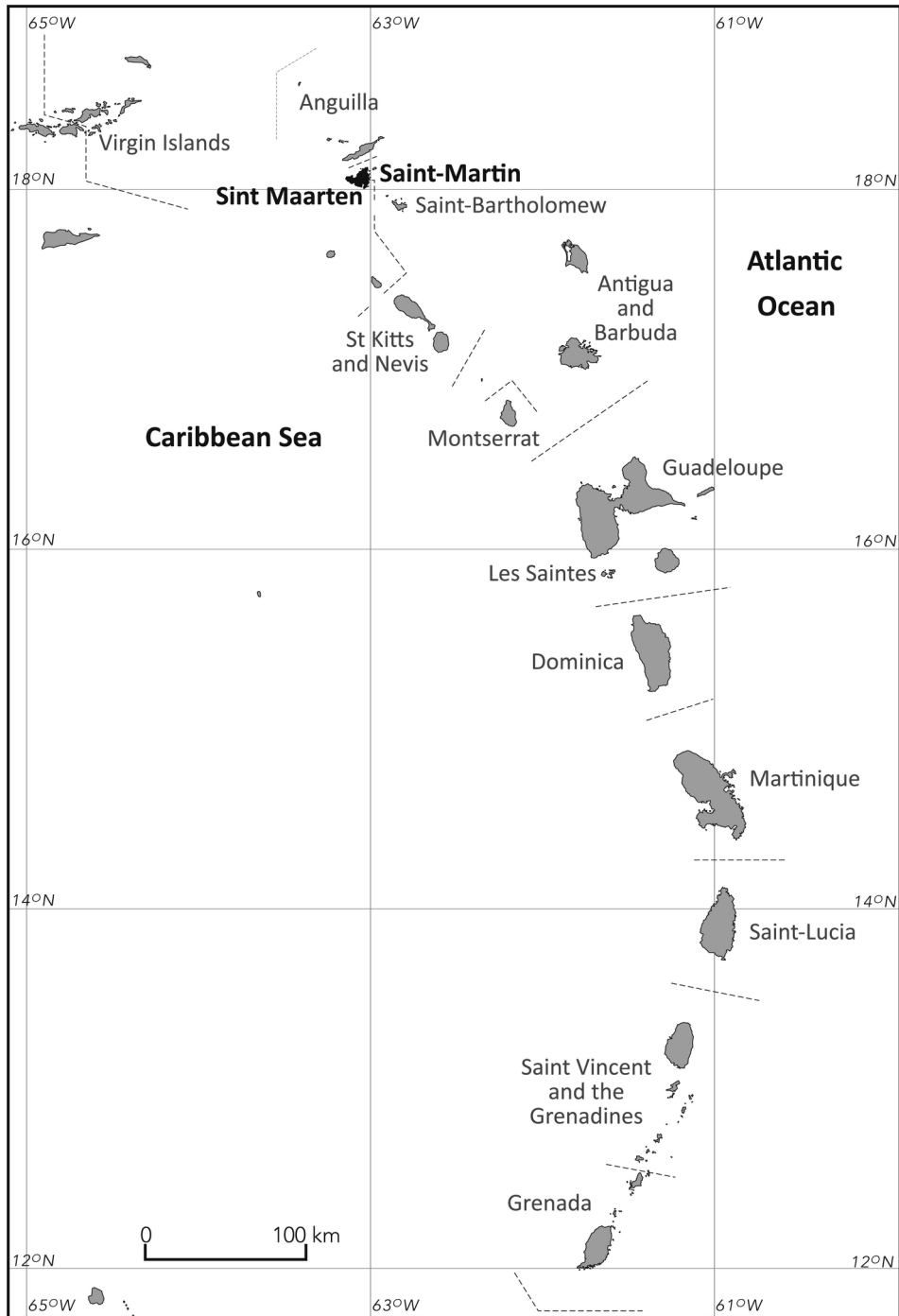








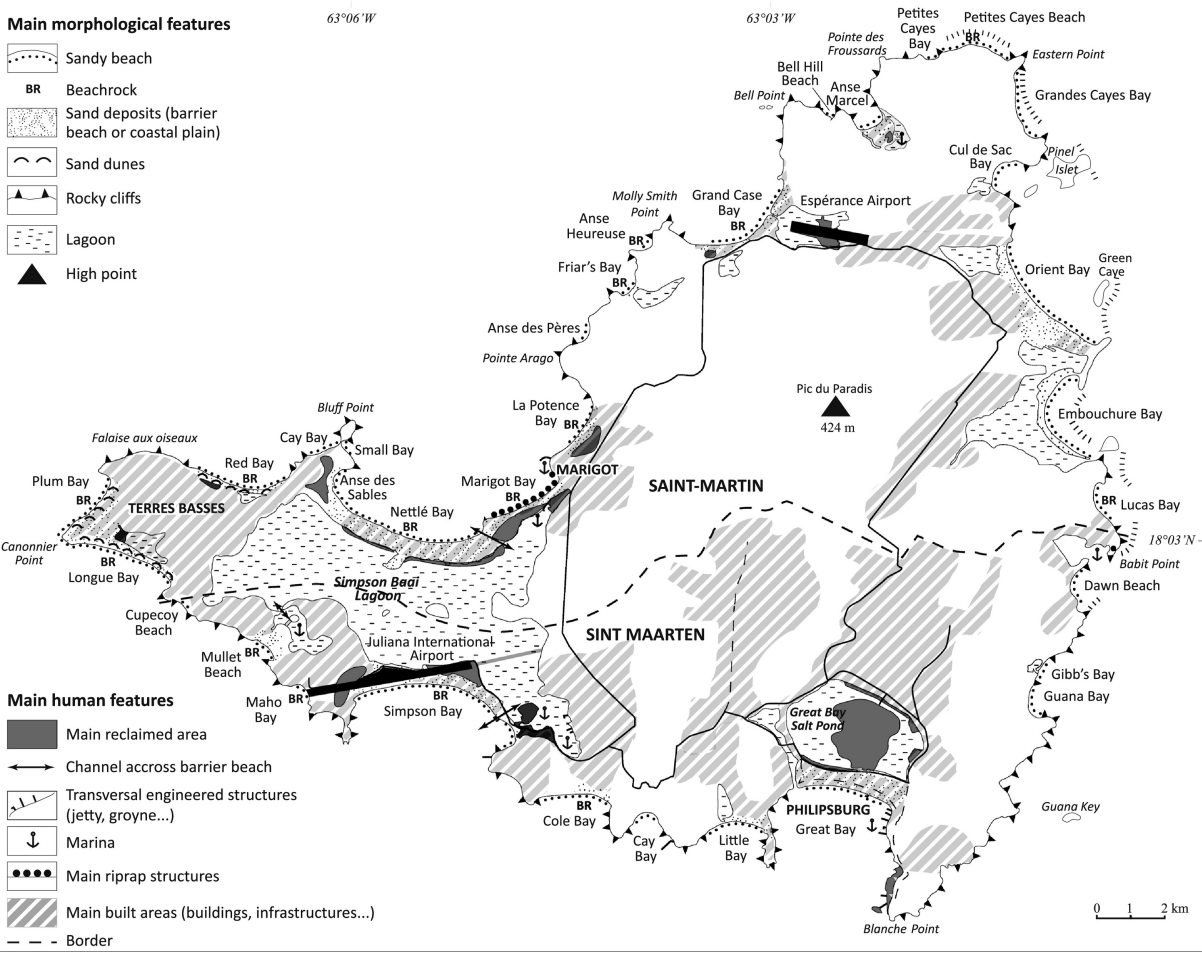
Figure 1

63°06' W

63°03' W

### Main morphological features

-  Sandy beach
- BR** Beachrock
-  Sand deposits (barrier beach or coastal plain)
-  Sand dunes
-  Rocky cliffs
-  Lagoon
-  High point



### Main human features


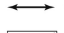



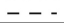

-  Main reclaimed area
-  Channel across barrier beach
-  Transversal engineered structures (jetty, groyne...)
-  Marina
-  Main riprap structures
-  Main built areas (buildings, infrastructures...)
-  Border

Figure 2

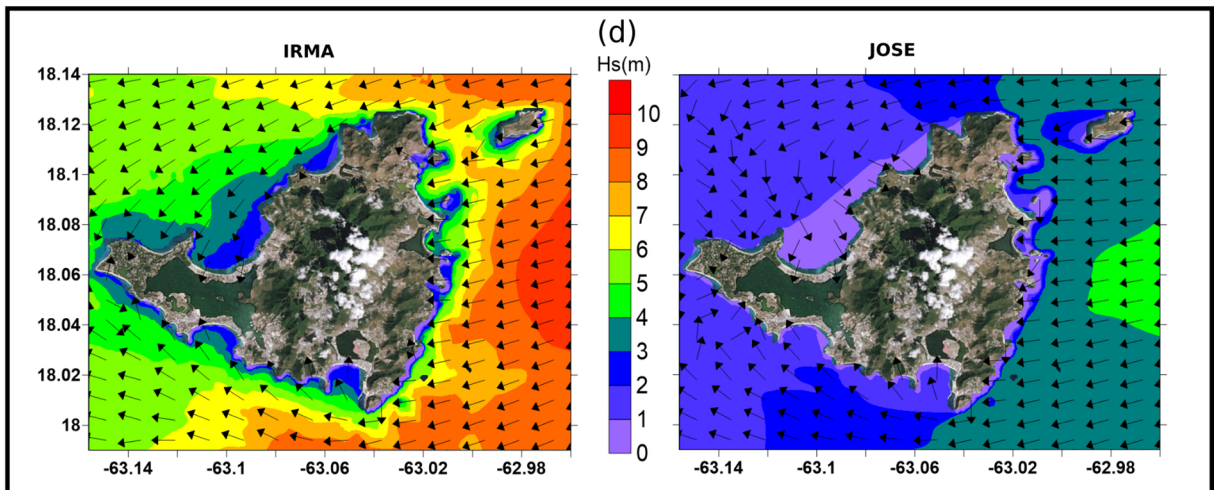
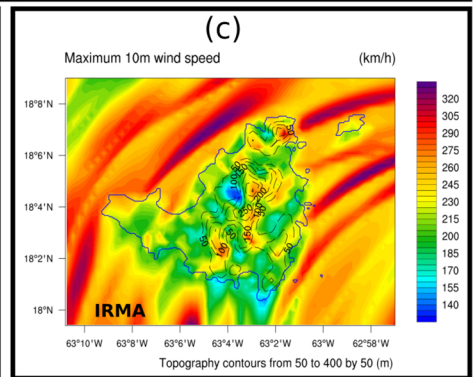
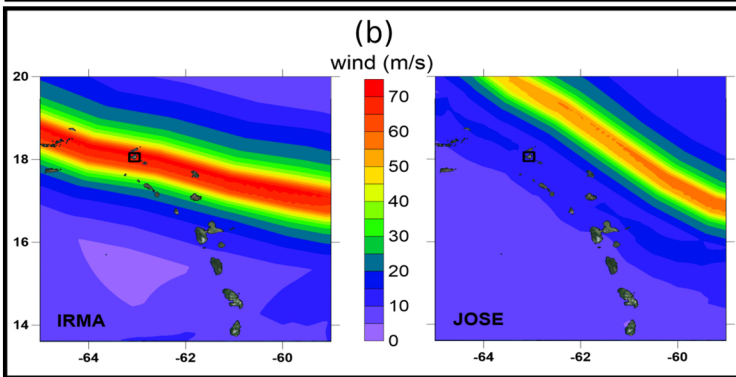
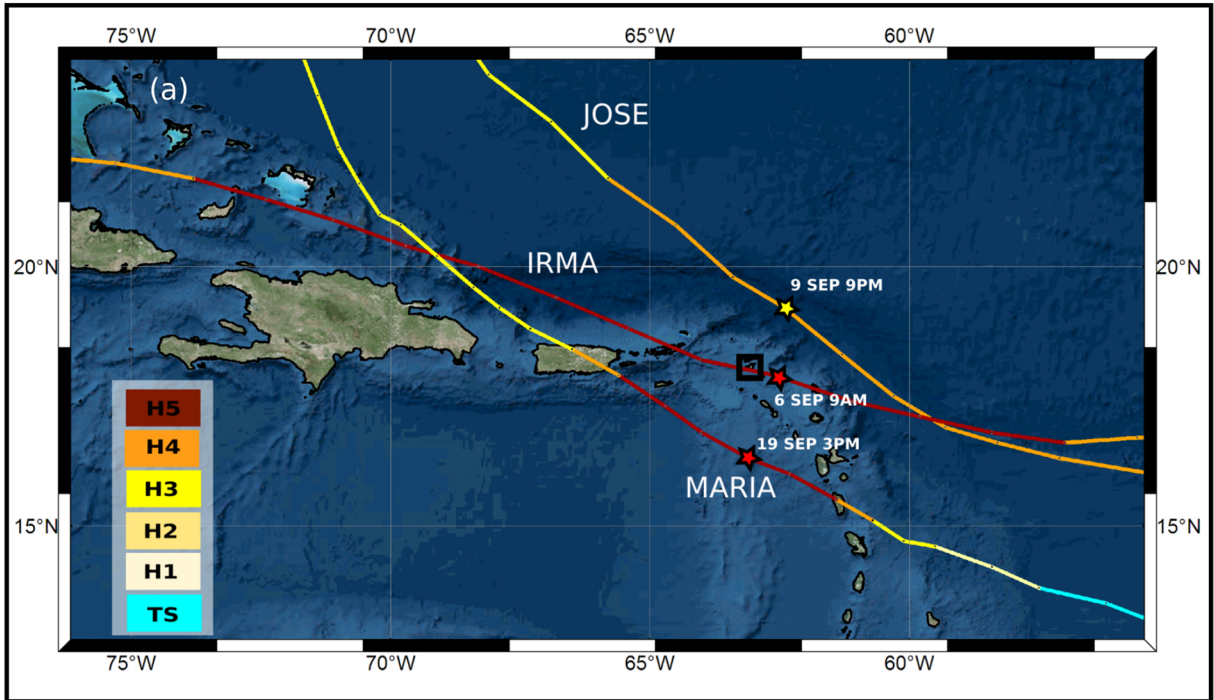
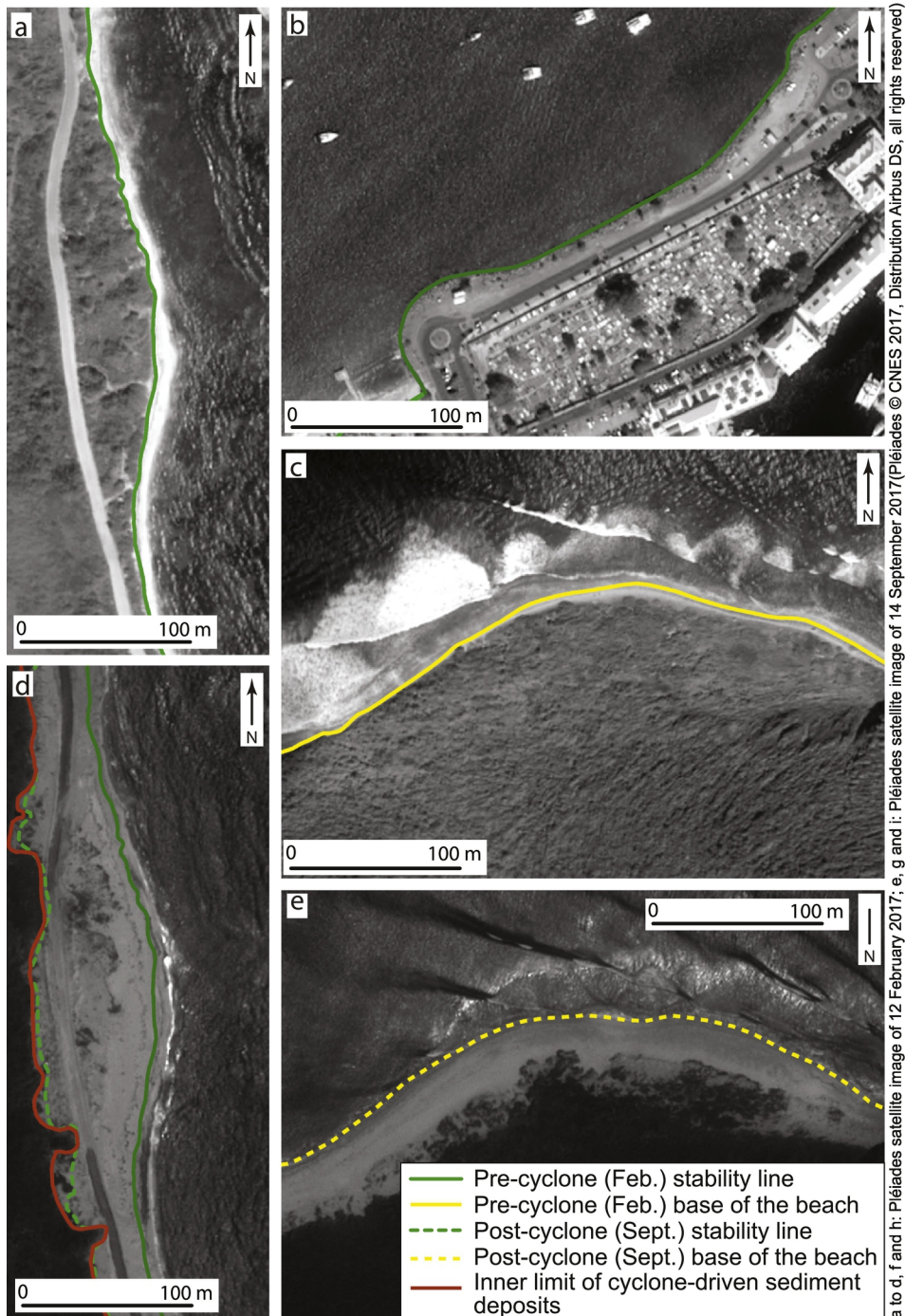


Figure 3



a to d, f and h: Pliades satellite image of 12 February 2017; e, g and i: Pliades satellite image of 14 September 2017 (Pliades © CNES 2017, Distribution Airbus DS, all rights reserved)

Figure 4

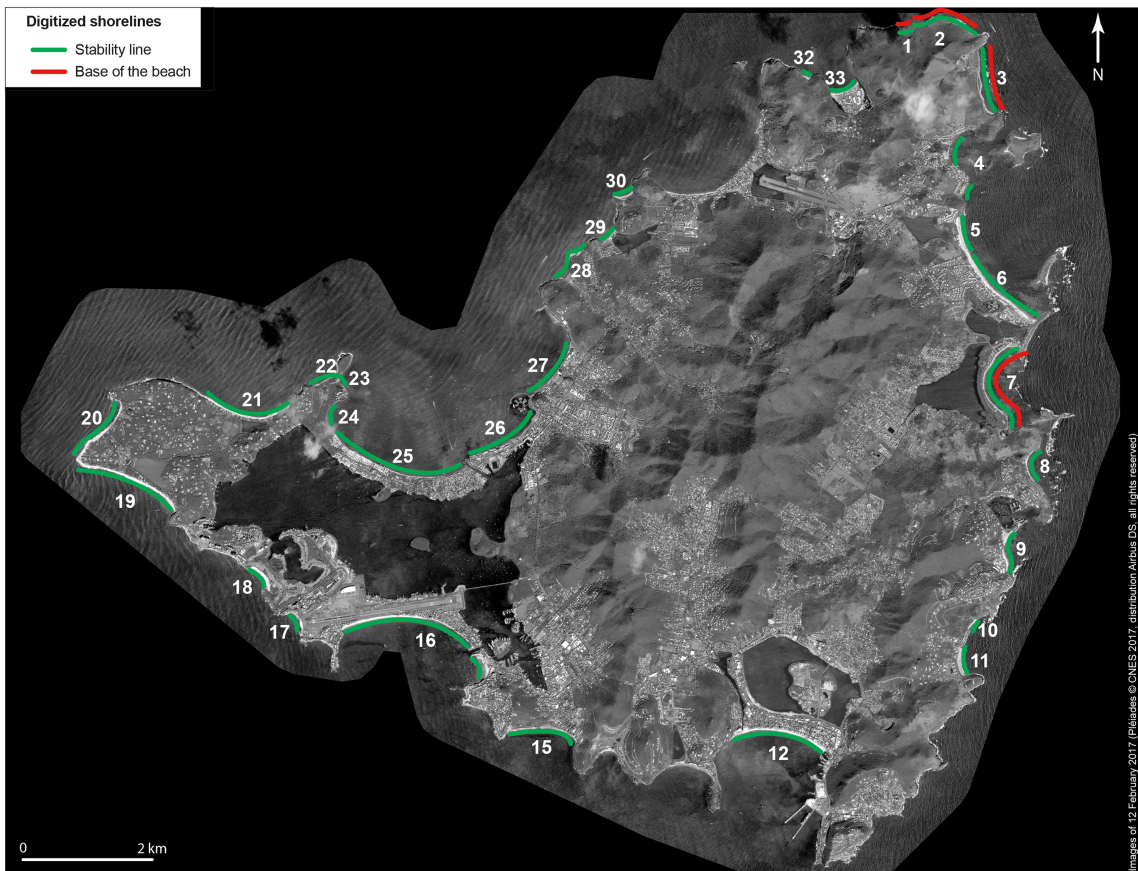


Figure 5

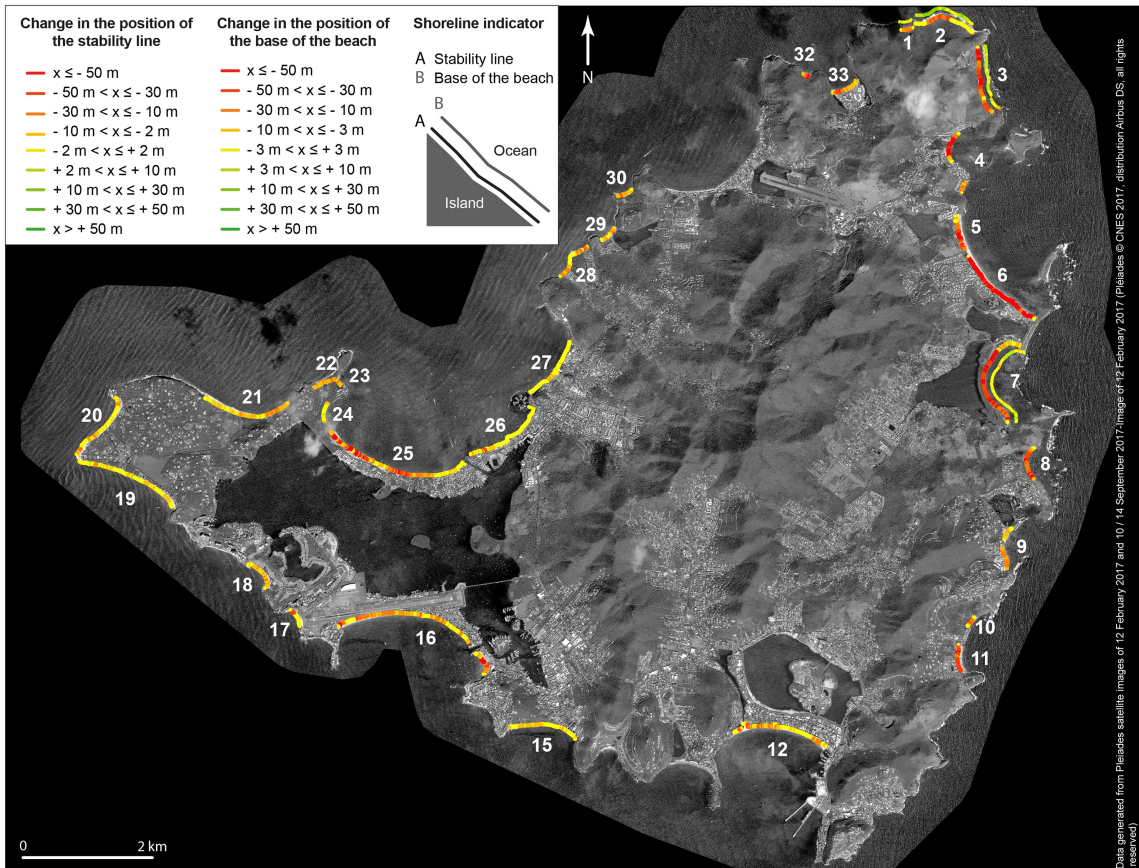


Figure 6

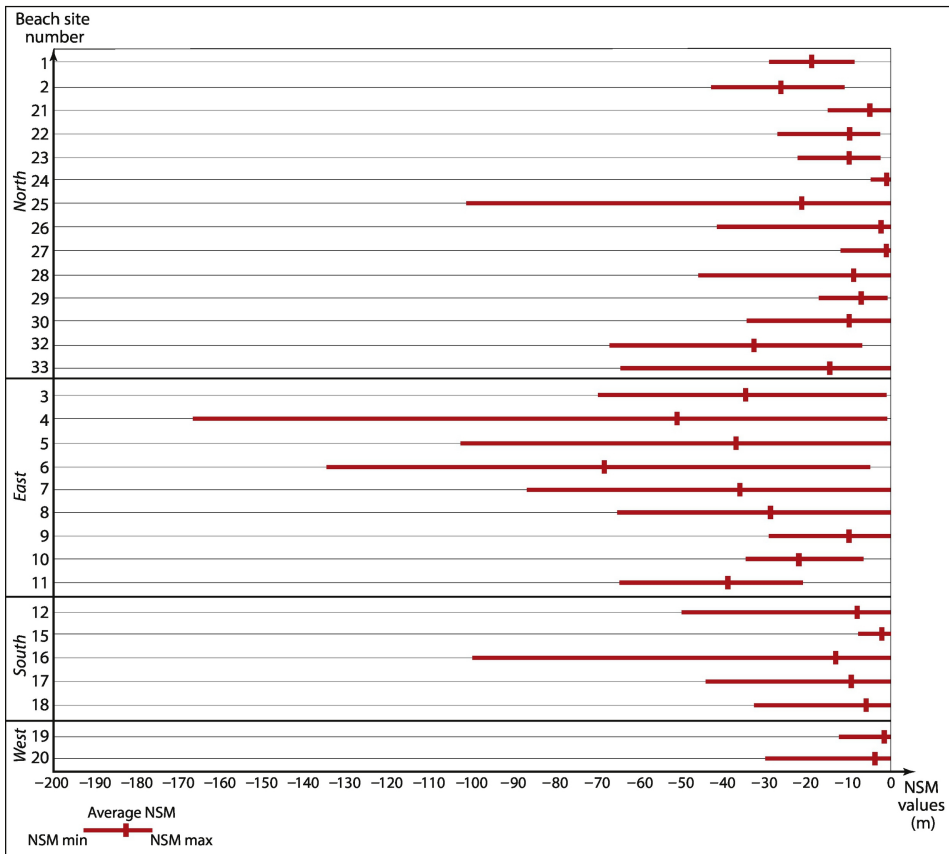


Figure 7

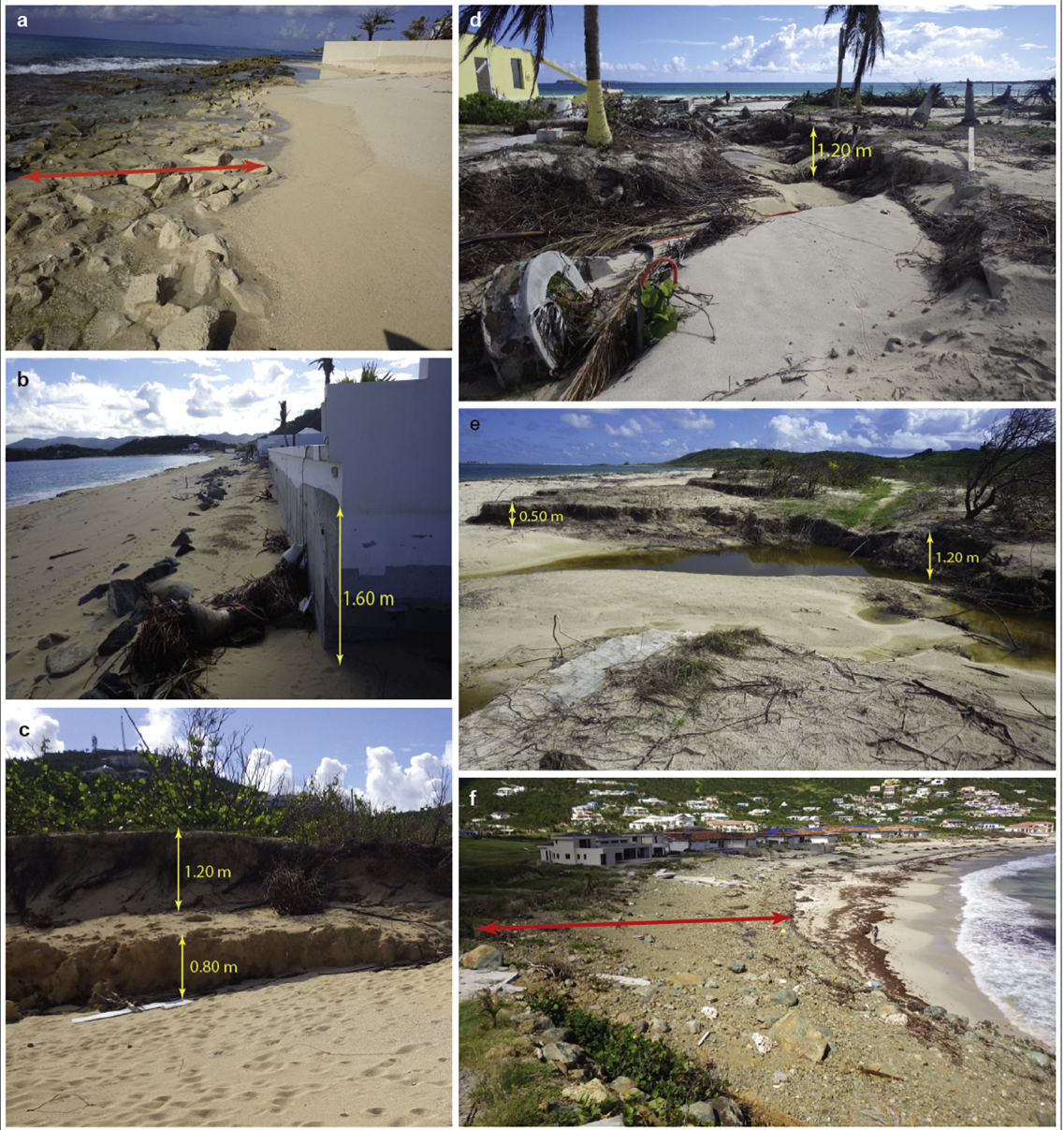


Figure 8





Figure 9

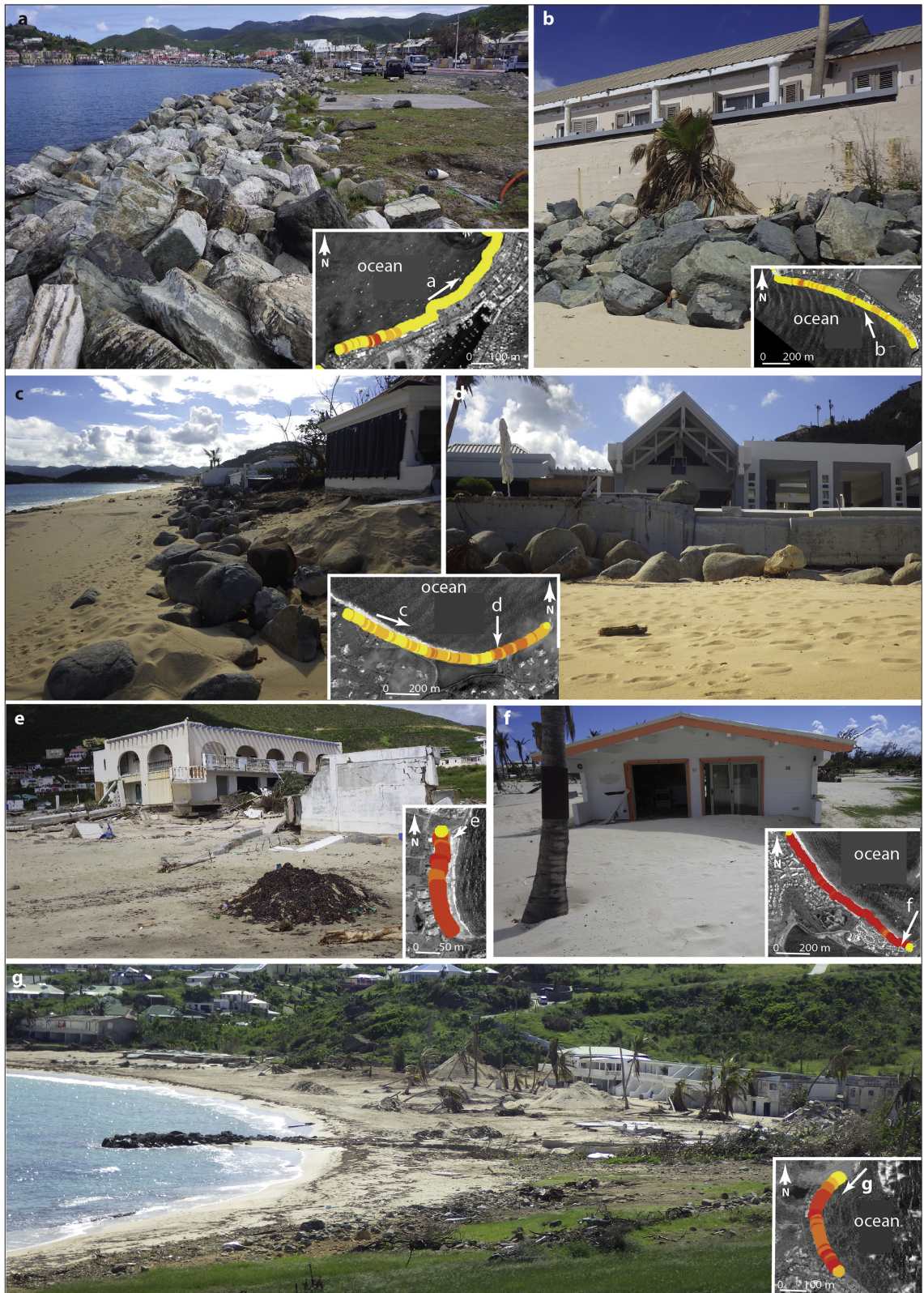
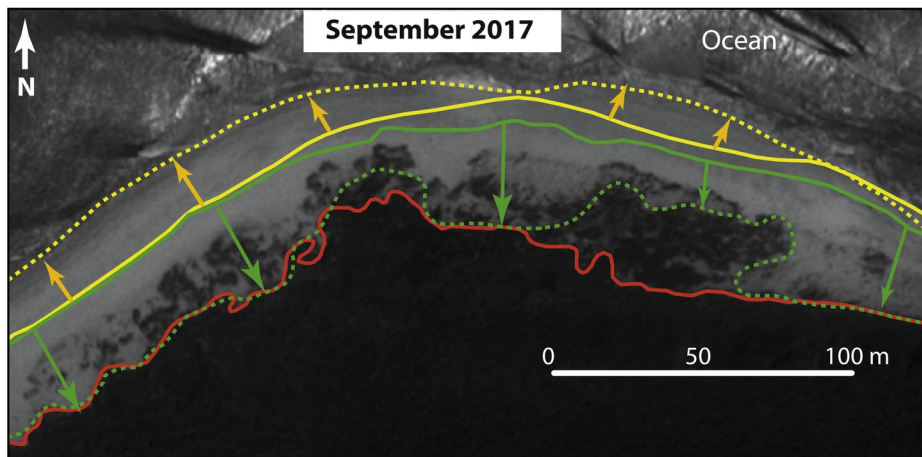
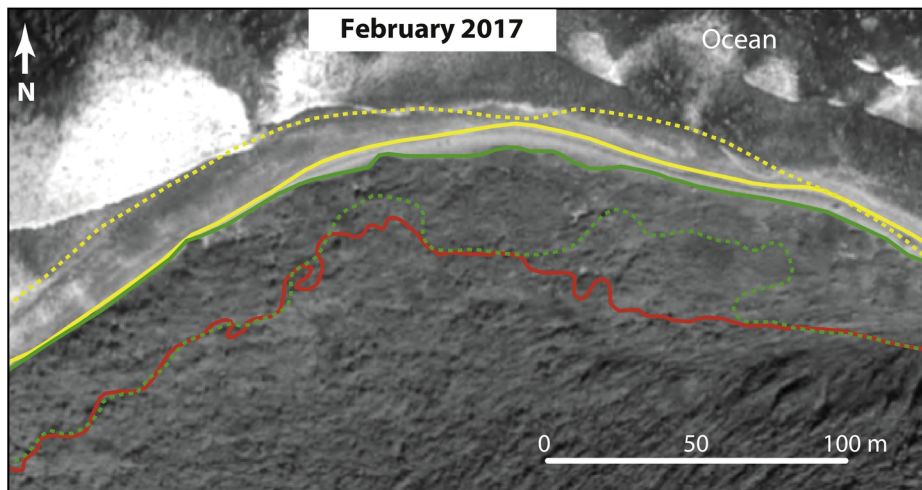
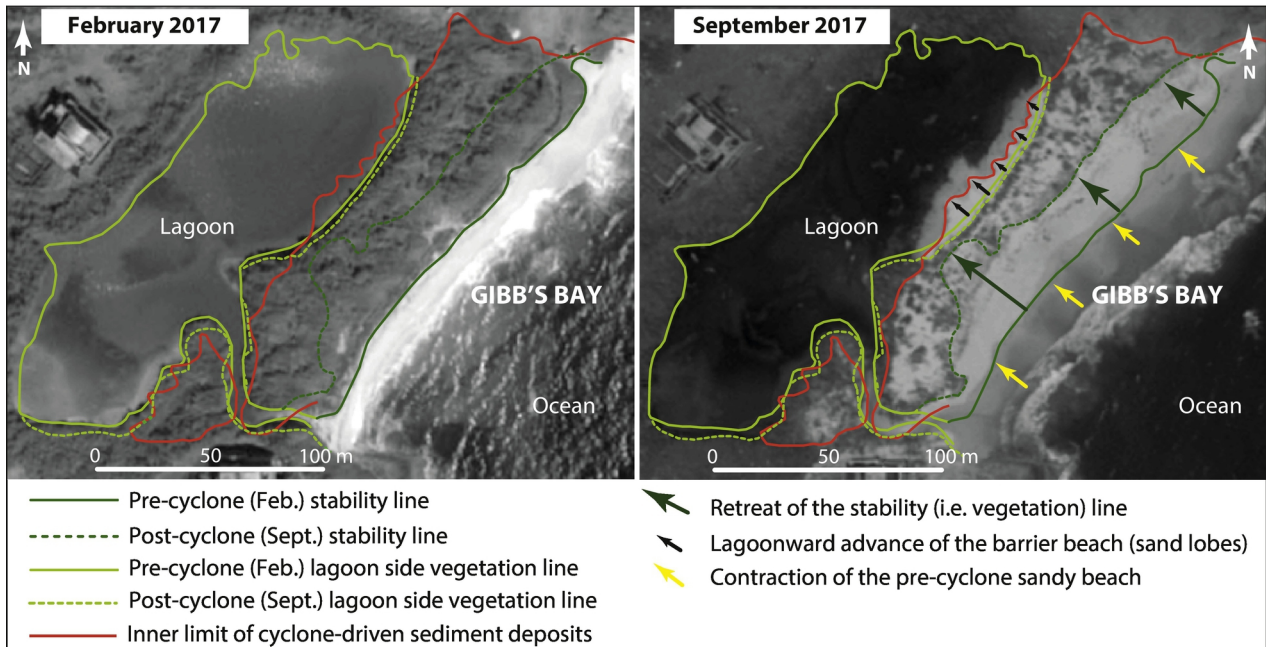


Figure 10



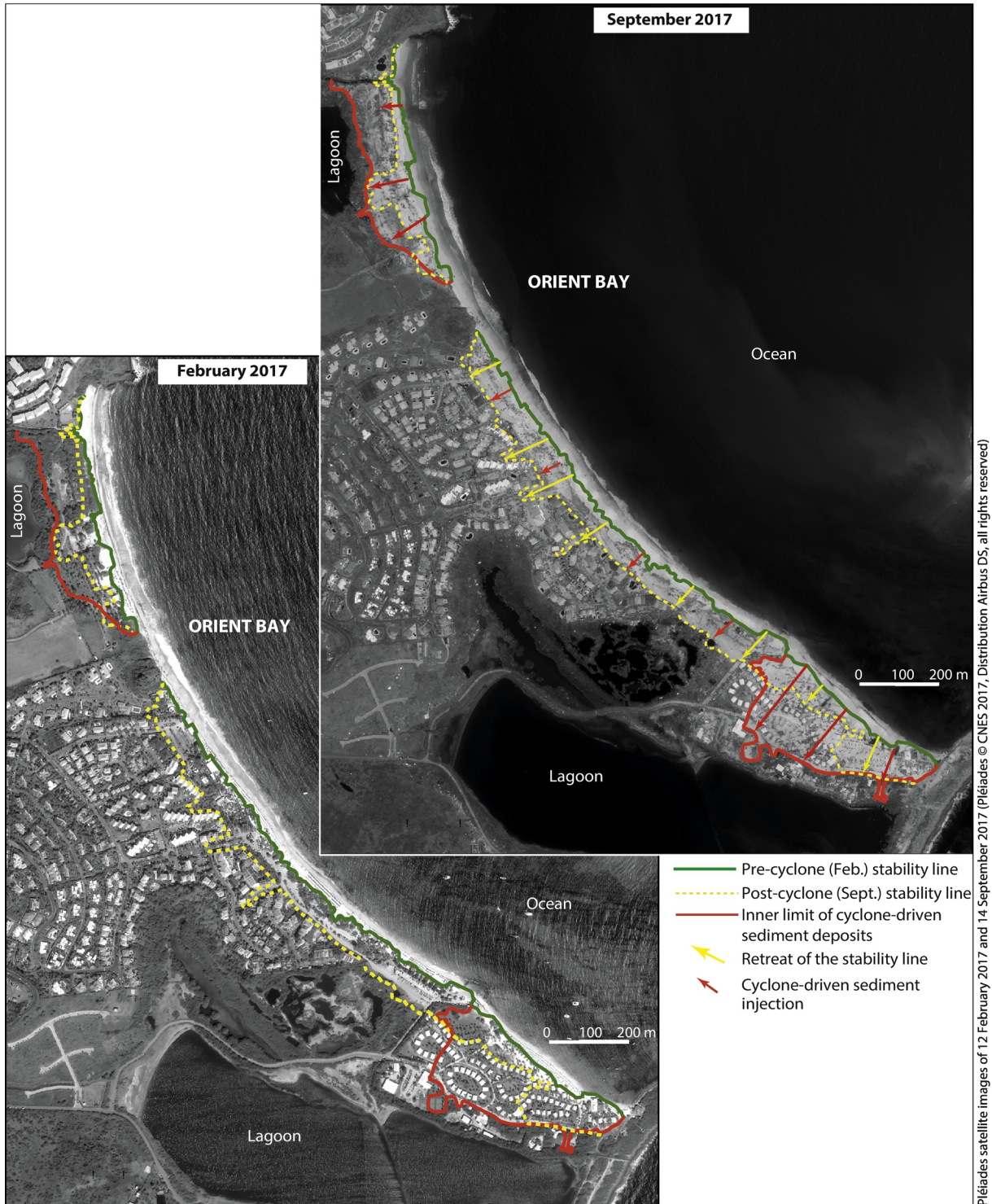
- Pre-cyclone (Feb.) base of the beach
- ⋯ Post-cyclone (Sept.) base of the beach
- Pre-cyclone (Feb.) stability line
- ⋯ Post-cyclone (Sept.) stability line
- Inner limit of cyclone-driven sediment deposits
- ↙ Retreat of the stability (i.e. vegetation) line
- ↗ Sandy beach expansion

Figure 11



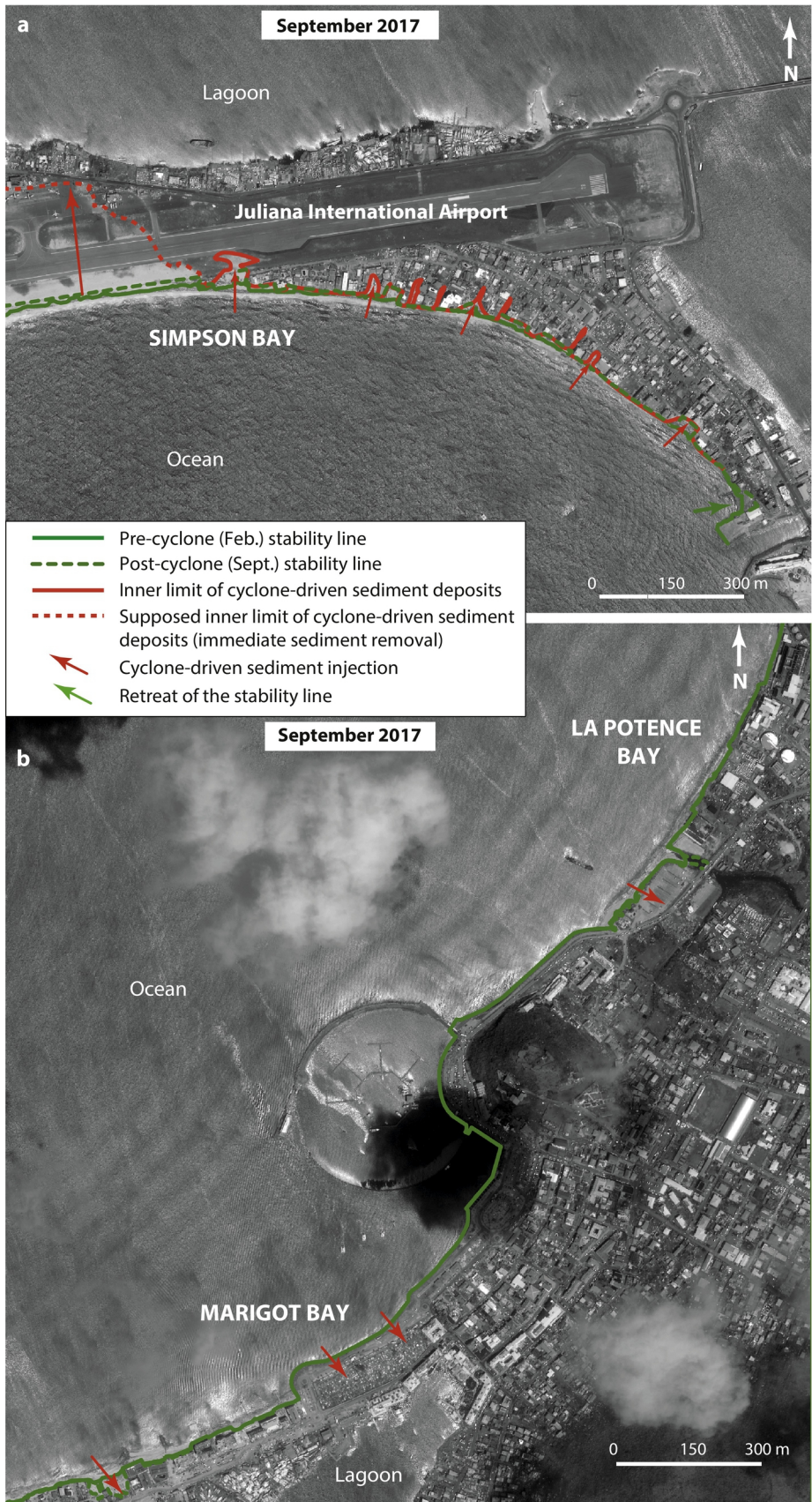
Pléiades satellite images of 12 February 2017 and 14 September 2017 (Pléiades © CNES 2017, Distribution Airbus DS, all rights reserved.)

Figure 12



Pleiades satellite images of 12 February 2017 and 14 September 2017 (Pleiades © CNES 2017, Distribution Airbus DS, all rights reserved)

Figure 13



Pléiades satellite images of 12 February 2017 and 14 September 2017 (Pléiades © CNES 2017, Distribution Airbus DS, all rights reserved)

Figure 14